

## Electronic Supporting Information

### Spontaneous mirror symmetry breaking in benzil-based soft crystalline, liquid crystalline cubic and isotropic liquid phases

Tino Reppe,<sup>a</sup> Silvio Poppe,<sup>a</sup> Xiaoqian, Cai,<sup>b</sup> Yu, Cao,<sup>b</sup> Feng Liu<sup>b\*</sup> and Carsten Tschierske<sup>a\*</sup>

<sup>a</sup> Institute of Chemistry, Martin Luther University Halle-Wittenberg, Kurt-Mothes-Straße 2, 06120 Halle, Germany. E-mail: carsten.tschierske@chemie.uni-halle.de

<sup>b</sup> State Key Laboratory for Mechanical Behaviour of Materials, Shaanxi International Research Center for Soft Matter, Xi'an Jiaotong University, Xi'an 710049, P.R. China. E-mail: feng.liu@xjtu.edu.cn

# Content

<b>1. Methods .....</b>	S3
<b>2. Additional Data .....</b>	S4
2.1 DSC traces .....	S4
2.2 Additional textures.....	S6
2.3 Additional XRD-data.....	S10
2.4 Structural data .....	S18
<b>3. Additional Figures.....</b>	S19
<b>4. Synthesis and Analytical Data.....</b>	S19
4.1 General.....	S19
4.2 General procedures .....	S20
4.3 Intermediates.....	S20
4.4 Compounds <b>2</b> and <b>4-6/n</b> .....	S21
4.5 Compounds <b>3/H</b> and <b>3/n</b> .....	S21
4.6 Representative NMR spectra .....	S26
<b>5. References .....</b>	S27

## 1. Methods

**Optical and calorimetric investigations.** Phase transitions were determined by polarizing microscopy (Leica DMR XP) in conjunction with a heating stage (FP 82 HT, Mettler) and controller (FP 90, Mettler) and by differential scanning calorimetry (DSC-7, Perkin Elmer) at heating/cooling rates of 10 K min<sup>-1</sup> (peak temperatures). If not otherwise noted transition temperatures and –enthalpies were taken from the second heating and cooling curve. Optical investigation was carried out under equilibrium conditions between glass slides which were used without further treatment, sample thickness was ~15 µm. A full wavelength retardation plate was used to determine the sign of birefringence. Optical micrographs were taken using a Leica MC120HD camera.

### X-ray diffraction.

**In-house measurements.** X-ray investigations (Kristalloflex 760H, Siemens) on powder-like samples were carried out using Ni filtered CuK $\alpha$  radiation (15 to 30 min exposure time). The samples were prepared in the isotropic state on a glass plate and cooled (rate: 5 K·min<sup>-1</sup>) to the measuring temperature. The samples were held on a temperature controlled heating stage and the diffraction patterns were recorded with a 2D detector (Vantec 500, Bruker); exposure time was 15-20 min. The sample-detector distance for the samples was 9.00 cm for WAXD and 26.90 cm for SAXD measurements. The diffraction patterns obtained were transform to 1D plots using GADDS over the full Chi range.

### Synchrotron XRD

**Synchrotron X-ray diffraction and electron density reconstruction.** - High-resolution small-angle powder diffraction experiments were recorded on Beamline BL16B1 at Shanghai Synchrotron Radiation Facility, SSRF. Samples were held in evacuated 1 mm capillaries. A Linkam hot stage with a thermal stability within 0.2 °C was used, with a hole for the capillary drilled through the silver heating block and mica windows attached to it on each side. A MarCCD detector was used.  $q$  calibration and linearization were verified using several orders of layer reflections from silver behenate and a series of  $n$ -alkanes. The measurement of the positions and intensities of the diffraction peaks is carried out using Galactic PeakSolve™ program, where experimental diffractograms are fitted using Gaussian shaped peaks. The diffraction peaks are indexed on the basis of their peak positions, and the lattice parameters and the plane/space groups are subsequently determined.

### The reconstructed electron density map of Cubic phases

The electron density  $E(xyz)$  can be generated by structural factor  $F(hkl)$  with Fourier transform

$$E(xyz) = \sum_{hkl} F(hkl) \exp[i2\pi(hx+ky+lz)] \quad (\text{Eqn. 1})$$

Here,  $F(hkl)$  is a complex number with real part  $A(hkl)$  and imaginary part  $B(hkl)$ .  $F(hkl)$  is related with observed scattering intensity  $I$ .

$$F(hkl) = |F(hkl)| \exp[i\phi(hkl)] = \sqrt{|I(hkl)|} \exp[i\phi(hkl)] \quad (\text{Eqn. 2})$$

Thus, the equation 1 can be rewritten as

$$E(xyz) = \sum_{hkl} \sqrt{|I(hkl)|} [A(hkl)\cos\phi(hkl) + B(hkl)\sin\phi(hkl)] \quad (\text{Eqn. 3})$$

Where  $\phi(hkl)$  is the phase. For centrosymmetric phase, e.g.  $Ia3d$ ,  $\phi(hkl)$  is either 0 or  $\pi$ , which makes it possible for a trial and error approach. The correct phase combination is determined by the proper physical merit.

However, for non-centrosymmetric phase, such as  $I23$ ,  $\phi(hkl)$  is arbitrary between 0 and  $\pi$ . Taking the model from a relevant work,<sup>S2</sup> we applied similar phases and intensity distributions on the phases we studied in this work.

## 2. Additional Data

### 2.1 DSC traces

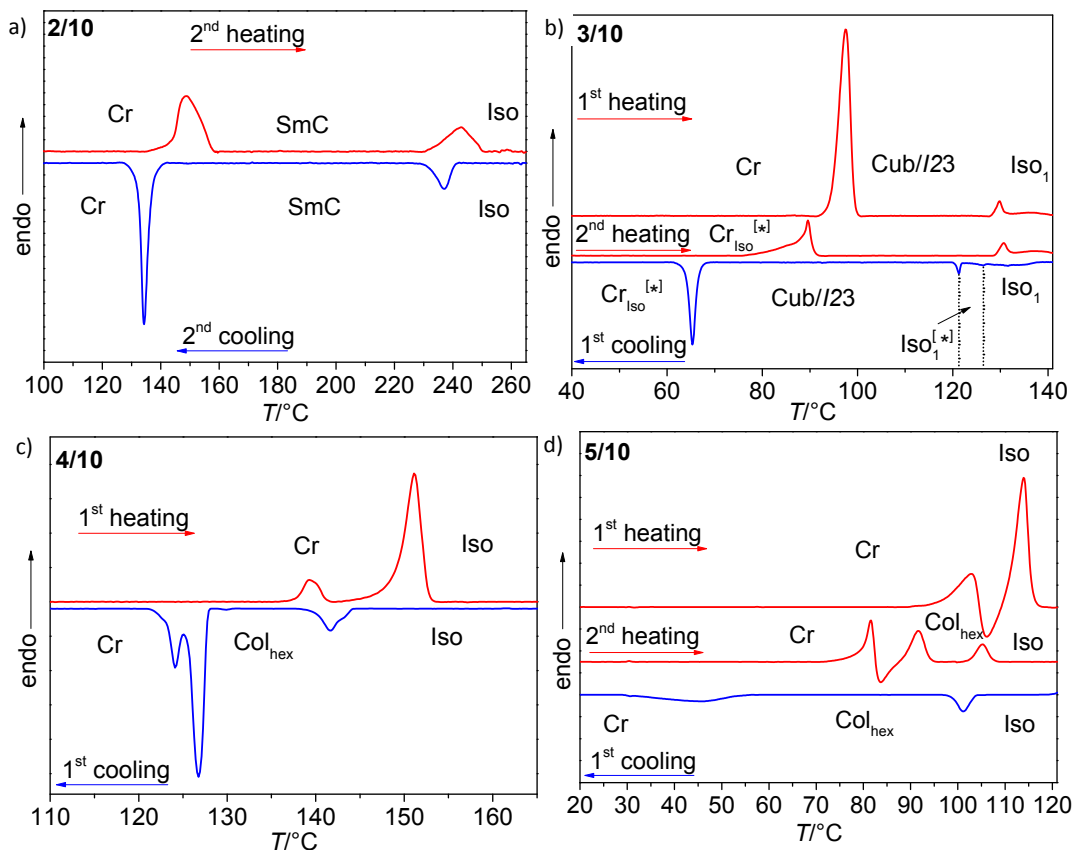


**Figure S1.** DSC heating and cooling traces of compounds **2/10-5/10** recorded at  $10 \text{ K min}^{-1}$ .

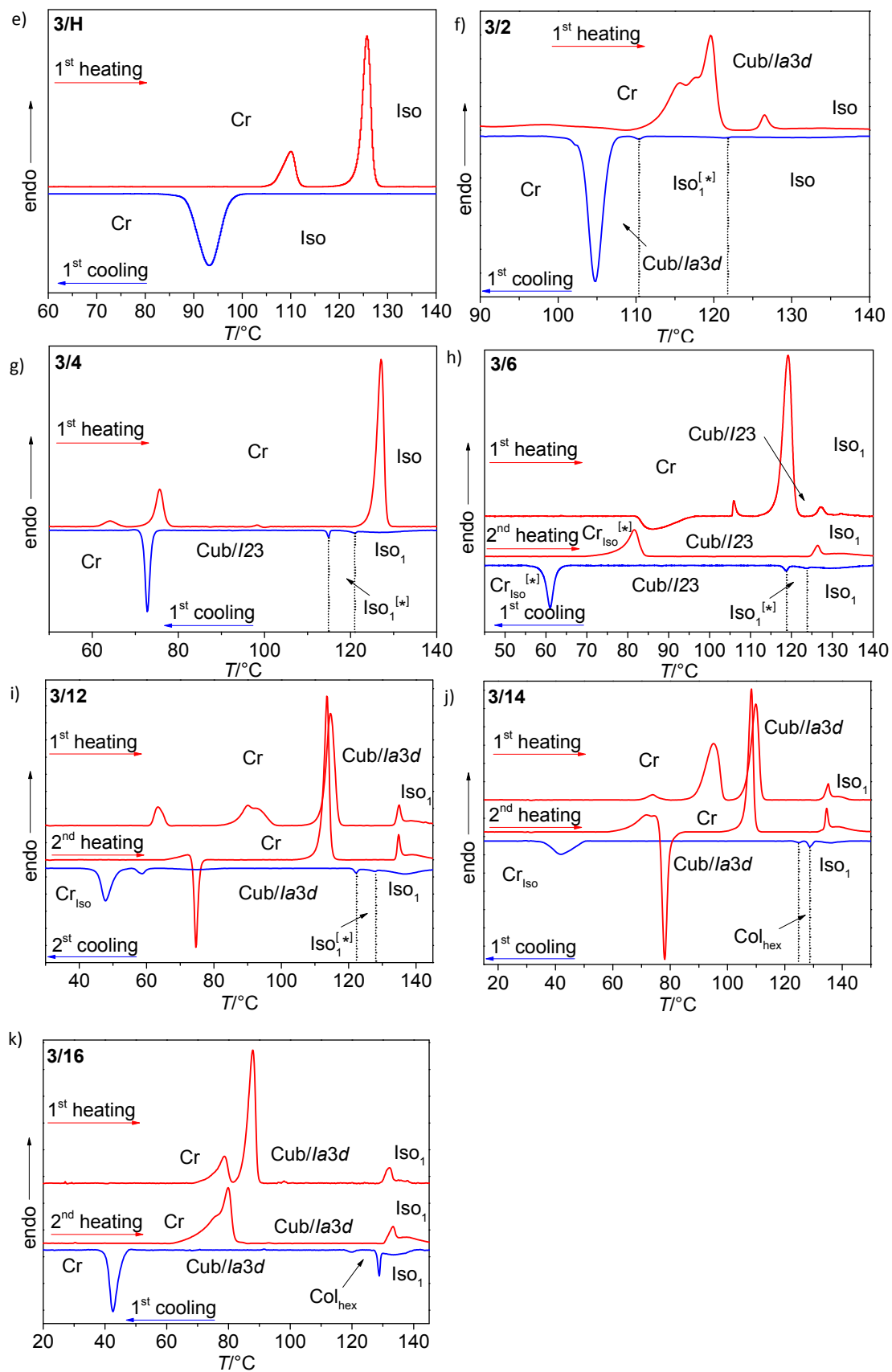


**Figure S1 (continued).** DSC heating and cooling traces of compounds **3/n** as recorded at 10 K min<sup>-1</sup>.

**Table S1.** Temperature ranges of the Iso-Iso<sub>1</sub> transitions.

<b>3/n</b>	heating	cooling
	<i>T/°C [ΔH kJ mol<sup>-1</sup>]</i>	<i>T/°C [ΔH kJ mol<sup>-1</sup>]</i>
<b>3/2</b>	Iso <sub>1</sub> 129-146 [2.8] Iso	Iso 144-122 [2.7] Iso <sub>1</sub>
<b>3/4</b>	-	Iso 140-123 [4.5] Iso <sub>1</sub>
<b>3/6</b>	Iso <sub>1</sub> 124-152 [5.7] Iso	Iso 149-116 [7.1] Iso <sub>1</sub>
<b>3/10</b>	Iso <sub>1</sub> 128-147 [5.7] Iso	Iso 144-120 [5.9] Iso <sub>1</sub>
<b>3/12</b>	Iso <sub>1</sub> 136-151 [6.2] Iso	Iso 150-129 [8.9] Iso <sub>1</sub>
<b>3/14</b>	Iso <sub>1</sub> 131-152 [7.2] Iso	Iso 153-120 [9.2] Iso <sub>1</sub>
<b>3/16</b>	135-148 [6.1] Iso	Iso 146-131 [6.0] Iso <sub>1</sub>

## 2.2 Additional textures

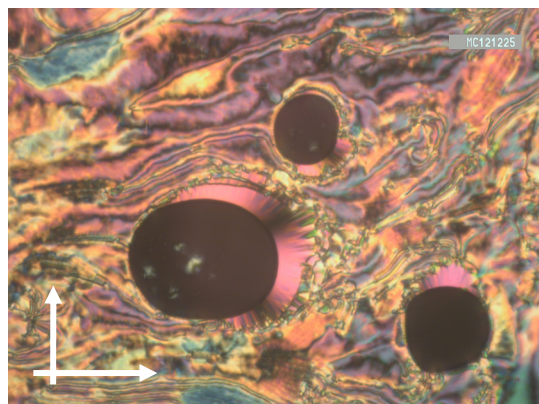


**Figure S2.** Textures of the (synclinic) SmC phase of **2/10** at 230 °C, showing the Schlieren texture and a fan-like texture around the air bubbles (black dots); the direction of the extinctions indicates a synclinic tilt of about 35 °; the arrows indicate the orientation of polarizer and analyzer; the width of the POM image is 0.8 mm.

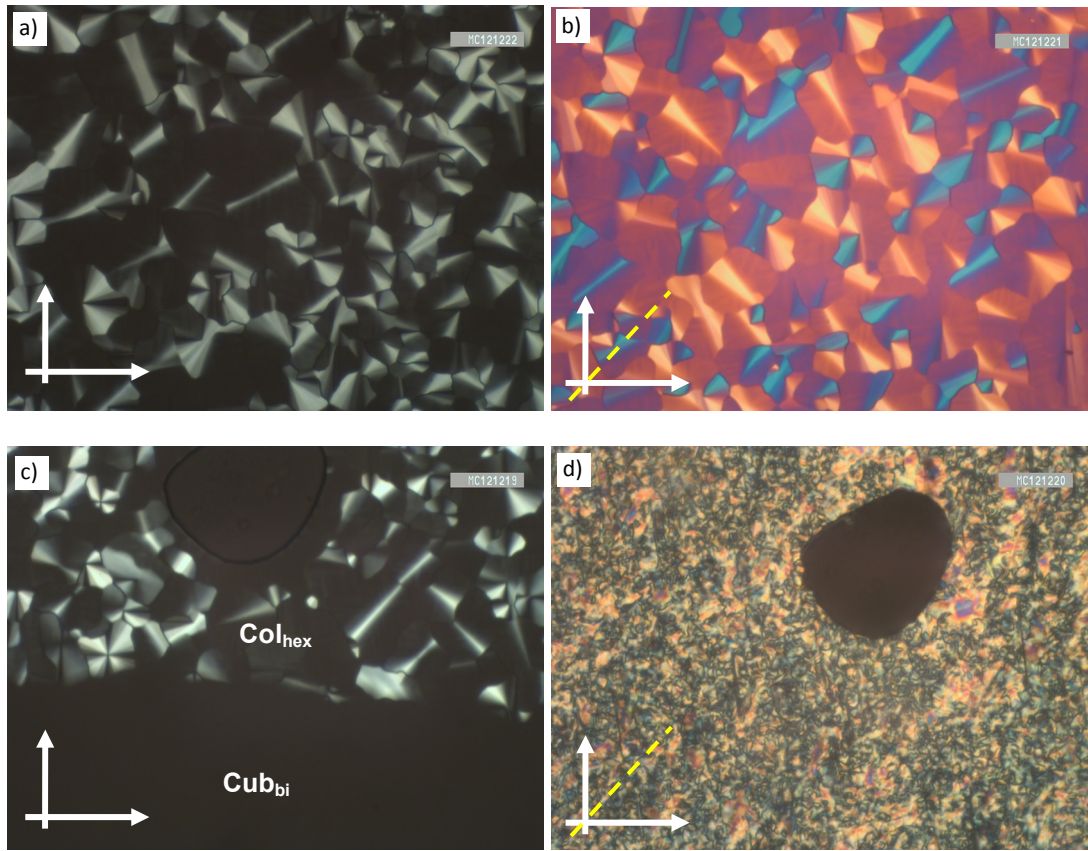


**Figure S3.** Textures of the  $\text{Col}_{\text{hex}}$  phase of **4/10** at  $142\text{ }^{\circ}\text{C}$ , a) between crossed polarizers (the dark areas represent homeotropic (optically isotropic) regions where the columns are perpendicular to the substrate surfaces, confirming the uniaxiality of the columnar phase) and b) with additional  $\lambda$ -retarder plate (the indicatrix direction is SW-NE), indicating negative birefringence and confirming an alignment of the  $\pi$ -conjugated aromatic cores with their long axes on average perpendicular to the column long axes; c) shows the transition to the  $\text{Cub}_{\text{bi}}/\text{Ia}\bar{3}d$  phase at  $T = 141\text{ }^{\circ}\text{C}$ , immediately followed by d) crystallization of the sample at the same temperature; the width of the POM images is 0.8 mm.

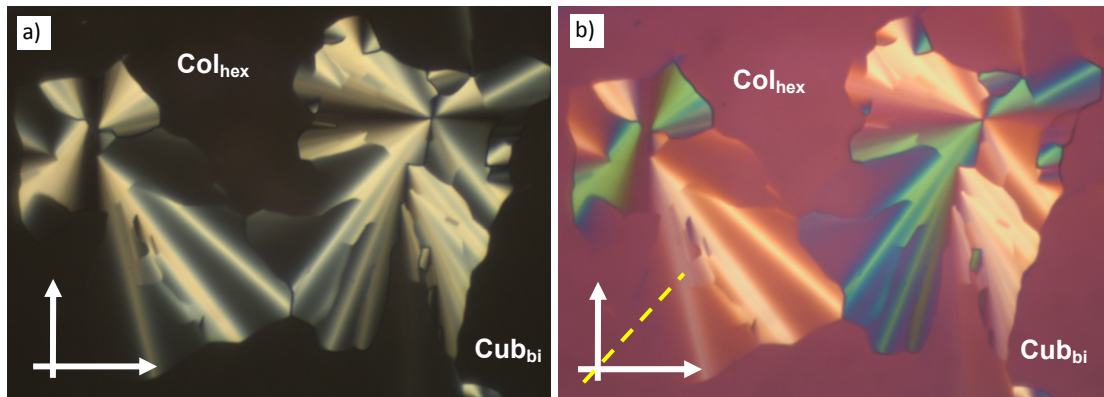


**Figure S4.** Textures of the  $\text{Col}_{\text{hex}}$  and  $\text{Cub}_{\text{bi}}/\text{Ia}\bar{3}d$  phases of **3/16** at  $123^{\circ}\text{C}$  a) between crossed polarizers (the dark at the left areas represent homeotropic (optically isotropic) regions where the columns are perpendicular to the substrate surfaces, confirming the uniaxiality of the columnar phase; the dark area at the right is the growing  $\text{Cub}_{\text{bi}}/\text{Ia}\bar{3}d$  phase) and b) with additional  $\lambda$ -retarder plate (the indicatrix direction, shown as yellow dotted line is SW-NE) indicating negative birefringence and confirming an alignment of the  $\pi$ -conjugated aromatic cores with their long axes on average perpendicular to the column long axes; the width of the POM images is 0.8 mm.

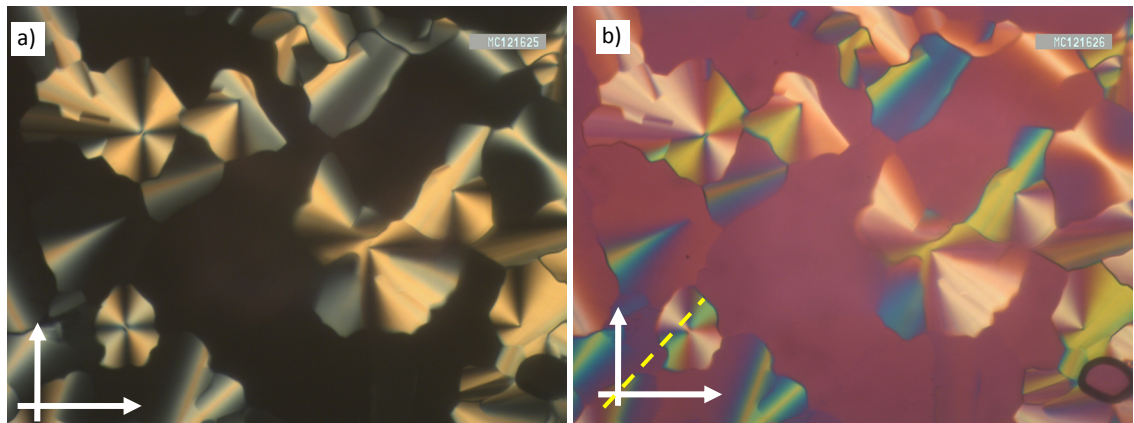


**Figure S5.** Textures of the  $\text{Col}_{\text{hex}}$  phase of **5/10** at  $100^{\circ}\text{C}$  a) between crossed polarizers (the dark at the left areas represent homeotropic (optically isotropic) regions confirming the uniaxiality of the columnar phase; b) with additional  $\lambda$ -retarder plate indicating negative birefringence. The width of the POM images is 0.8 mm.

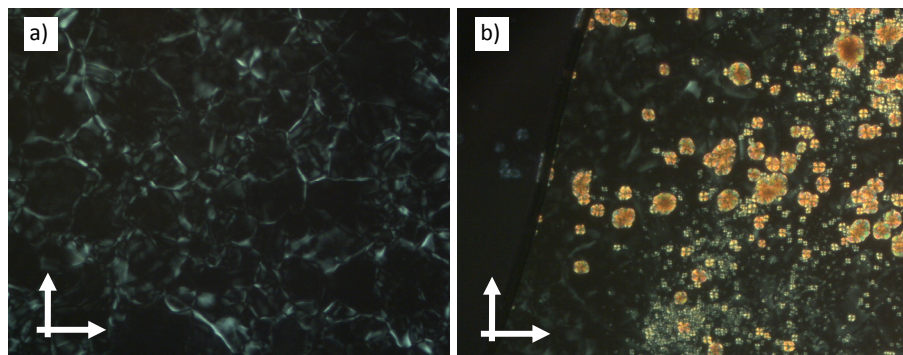


**Figure S6.** a) Achiral  $\text{Cr}_{\text{Iso}}$  phase of **3/12** at 35 °C; the weak birefringence, occurring already in the  $\text{Cub}_{\text{bi}}/\text{Ia}\overline{3}d$  phase at 80 °C is most likely due to a strain between the cubic domains arising on cooling; b) shows the crystallization of the birefringent Cr phase from the  $\text{Cr}_{\text{Iso}}$  phase of **3/14**; the width of the POM images is 0.8 mm.

## 2.3 Additional XRD-data

### 2.3.1 Cub<sub>bi</sub> phases

**Table S2.** SAXS data of the Cub<sub>bi</sub>/Ia $\bar{3}d$  phases of the investigated compounds.

Compd.	( <i>hkl</i> )	<i>d</i> <sub>obs</sub> – spacing/nm	<i>d</i> <sub>calc</sub> – spacing/nm	<i>d</i> <sub>obs</sub> – <i>d</i> <sub>calc</sub>	<i>a</i> <sub>cub</sub> /nm ( <i>T</i> /°C)
<b>3/2</b>	(211)	5.28	5.28	0.00	12.92 (122)
	(220)	4.60	4.57	0.03	
<b>3/12</b>	(211)	4.65	4.65	0.00	11.38 (125)
	(220)	4.05	4.02	0.03	
<b>3/14</b>	(211)	4.63	4.63	0.00	11.34 (125)
	(220)	4.03	4.01	0.02	
<b>3/16</b>	(211)	4.70	4.70	0.00	11.51 (120)
	(220)	4.10	4.07	0.03	

**Table S3.** SAXS data of Cub<sub>bi</sub>/I23<sup>[\*]</sup> phases of the investigated compounds.

Compd.	( <i>hkl</i> )	<i>d</i> <sub>obs</sub> – spacing/nm	<i>d</i> <sub>calc</sub> – spacing/nm	<i>d</i> <sub>obs</sub> – <i>d</i> <sub>calc</sub>	<i>a</i> <sub>cub</sub> /nm ( <i>T</i> /°C)
<b>3/4</b>	(321)	4.92	4.92	0.00	18.39 (110)
	(400)	4.55	4.60	0.05	
	(420)	4.06	4.11	0.05	
<b>3/6</b>	(321)	4.84	4.84	0.00	18.12 (123)
	(400)	4.54	4.53	0.01	
	(420)	4.13	4.05	0.08	
<b>3/10</b>	(321)	4.92	4.92	0.00	18.42 (110)
	(400)	4.57	4.60	0.03	
	(420)	4.16	4.12	0.04	

**Table S4.** Experimental and calculated *d*-spacings, relative integrated intensities for the Cub/*I*23<sup>[\*]</sup> phase of **3/4** at 110 °C from synchrotron-based SAXS. All intensities values are Lorentz and multiplicity corrected. The phases and intensities used in the reconstruction of the electron density map of the Cub<sub>bi</sub>/*I*23 phase is based on the results from reference S2.

( <i>hkl</i> )	<i>d</i> <sub>obs.-</sub> spacings (nm)	<i>d</i> <sub>cal.-</sub> spacings (nm)	<i>intensity</i>	<i>phase</i>
(110)	12.88	12.98	0.01	/
(211)	7.48	7.49	0.06	/
(220)	6.48	6.49	0.09	/
(310)	5.80	5.80	0.77	0
(222)	5.30	5.30	9.68	-0.24π
(321)	4.90	4.90	30.21	-0.91π
(312)			66.83	-0.59π
(400)	4.59	4.59	100.00	0
(330)	4.33	4.33	1.81	0
(411)			1.71	-0.81π
(420)	4.11	4.10	15.54	0
(332)	3.91	3.91	0.06	/
(422)	3.75	3.75	1.05	/
(431)	3.60	3.60	0.38	/
(510)			0.75	/
(432)	3.35	3.41	0.24	/
(440)	3.25	3.24	0.06	/
(433)	3.15	3.15	0.12	/
(530)			0.12	/
(442)	3.06	3.06	0.10	/
(600)			0.41	/
(532)	2.98	2.98	0.10	/
(611)			0.21	/
(620)	2.91	2.90	0.05	/
(541)	2.84	2.83	0.17	/
(622)	2.77	2.77	0.02	/

(631)	2.71	2.71	0.11	/
(444)	2.65	2.65	0.84	/
(543)			0.03	/
(550)	2.60	2.60	0.10	/
(710)			0.05	/
(640)	2.55	2.54	0.23	/
(552)			0.24	/
(633)	2.50	2.50	0.24	/
(721)			0.12	/
(642)	2.46	2.45	0.02	/
(730)	2.41	2.41	0.04	/
(651)			0.01	/
(732)	2.33	2.33	0.01	/
(800)	2.26	2.29	0.39	/
(660)	2.14	2.16	0.09	/
(840)	2.03	2.05	0.05	/
(833)			0.02	/
(910)	2.00	2.03	0.02	/
(842)	1.98	2.00	0.02	/
(655)			0.01	/
(761)	1.96	1.98	0.01	/
(664)	1.94	1.96	0.08	/
(844)	1.86	1.87	0.05	/
(770)	1.84	1.85	0.06	/
(860)	1.82	1.84	0.04	/
(862)	1.79	1.80	0.01	/
$a_{\text{cub}} = 18.35 \text{ nm}$				

**Table S5.** Experimental and calculated  $d$ -spacings, relative integrated intensities, and phases used in the reconstruction of electron densities for the Cub/ $Ia\bar{3}d$  phase of **3/16** at 110°C from synchrotron-based SAXS. All intensities values are Lorentz and multiplicity corrected.

( $hkl$ )	$d_{\text{obs.}}$ - spacings (nm)	$d_{\text{cal.}}$ - spacings (nm)	intensity	phase
(211)	4.74	4.74	100.00	$\pi$
(220)	4.11	4.11	25.94	$\pi$
(321)	3.11	3.11	0.06	0
(400)	2.91	2.91	1.07	$\pi$
(332)	2.48	2.48	0.41	$\pi$
(422)	2.38	2.37	0.46	0
(532)	1.89	1.89	0.03	/
(611)			0.05	/
(543)	1.64	1.64	0.03	/
$a_{\text{cub}} = 11.62 \text{ nm}$				

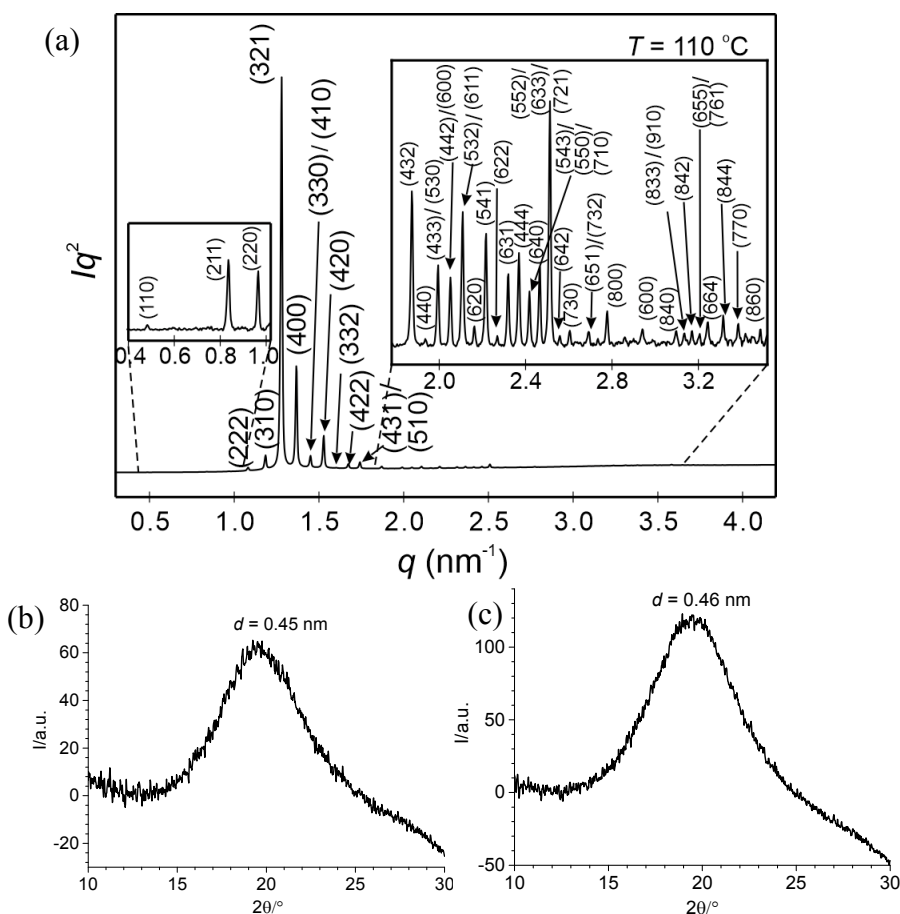


**Figure S7.** a) and b) SAXS/WAXS diffractogram of the  $I23^{[*]}$  phase of **3/4** at 110 °C; c) WASX diffractogram of the  $Ia\bar{3}d$  phase of **3/16** at 120 °C.

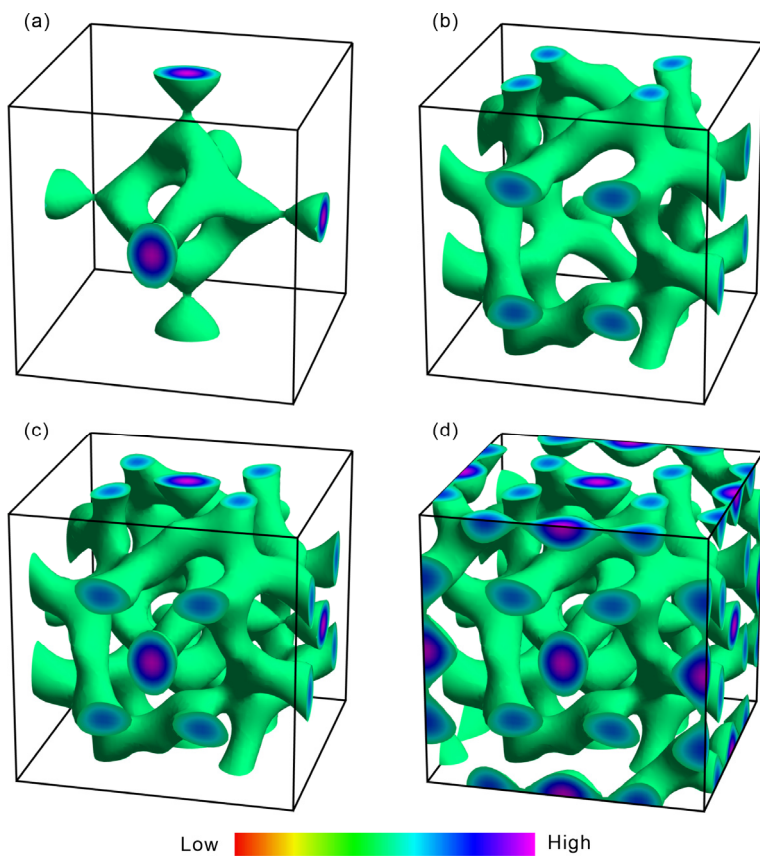


**Figure S8.** Reconstructed electron density maps of the triple network cubic phase with space group symmetry  $I\bar{2}3$ . The green isosurfaces enclose the high electron density (blue/purple, aromatic cores) regions of the 3D electron density map: (a) Inner network; (b) middle network; (c) inner and middle networks; (d) inner, middle and outer networks. The low electron density (red/yellow, alkyl chains) regions are omitted for clarifying the networks.

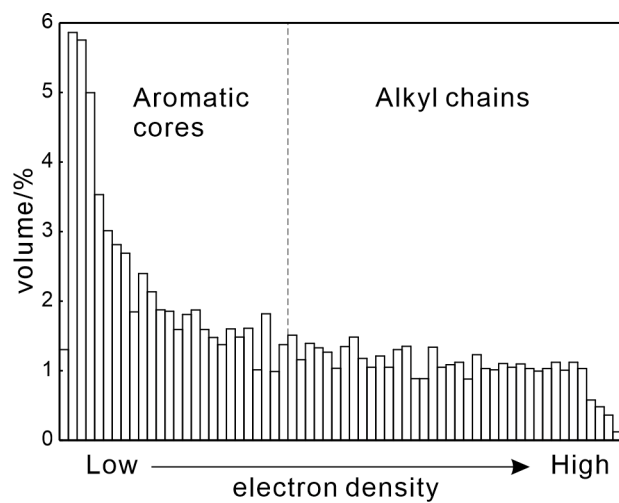


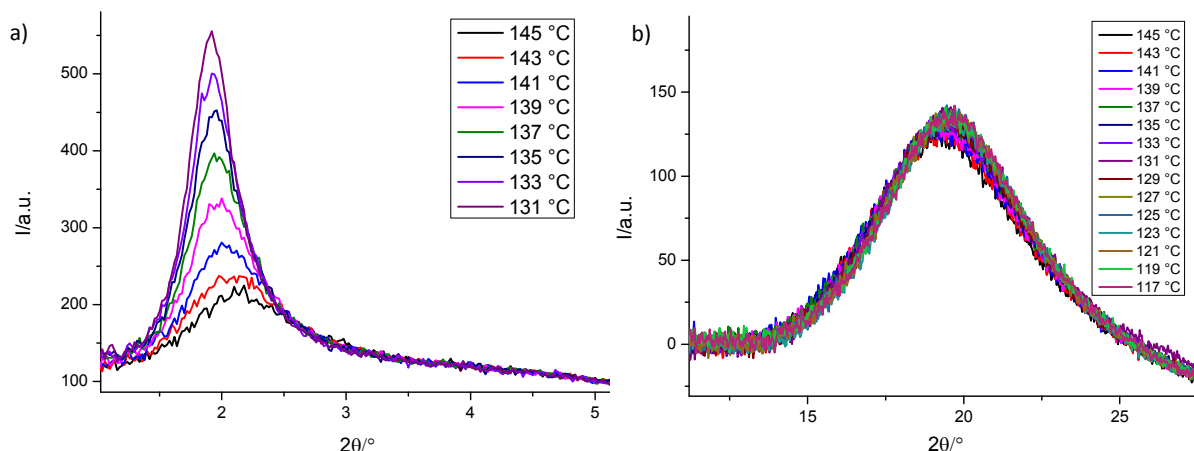
**Figure S9.** The electron density histogram of the  $Ia\bar{3}d$  phase of compound **3/16**, calculated based on the phase combination listed in Table S5. The volume ratio of high and low electron density region is 0.4:0.6 for aromatic cores and alkyl tails, respectively.

### 2.3.2 Smectic and columnar phases

**Table S6.** SAXS data of the smectic and columnar phases.

Compd.	Phase	(hk)	$d_{\text{obs}} - \text{spacing}/\text{nm}$	$a/\text{nm}$ ( $T/\text{^{\circ}C}$ )
<b>2/10</b>	SmC	10	3.66	3.66 (170)
<b>3/14</b>	Col <sub>hex</sub>	10	4.41	5.09 (131)
<b>5/10</b>	Col <sub>hex</sub>	10	4.39	4.39 (95)

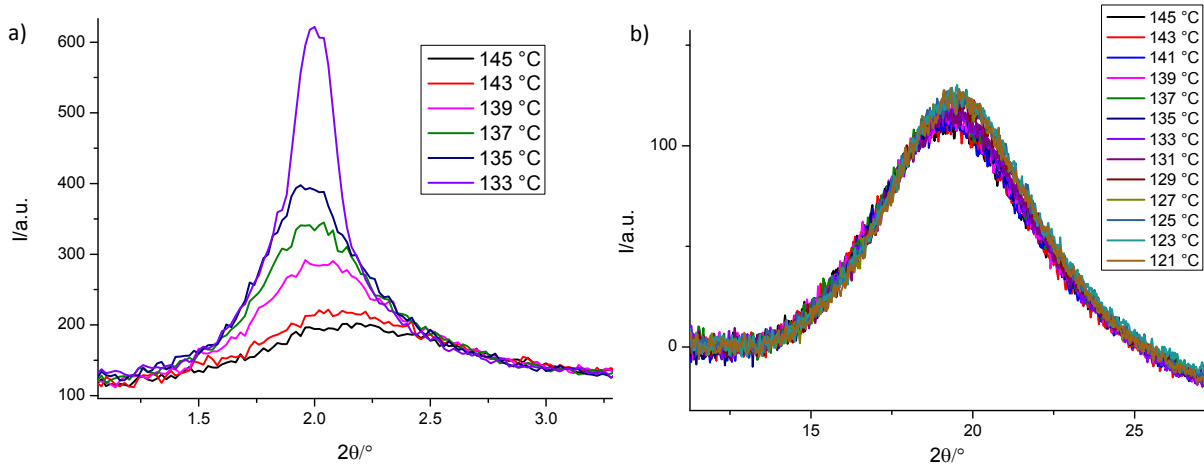
### 2.3.3 Isotropic mesophases



$T/\text{^{\circ}C}$	$2\theta/\text{^{\circ}}$	$\theta/\text{^{\circ}}$	$\theta/\text{rad}$	$d/\text{nm}$	$\text{FWHM}/\text{^{\circ}}$	$\zeta/\text{nm}$
145	2.203	1.101	0.019	4.011	0.81	24
143	2.132	1.066	0.019	4.143	0.73	25
141	2.075	1.038	0.018	4.257	0.64	27
139	2.023	1.011	0.018	4.368	0.58	29
137	1.987	0.994	0.017	4.445	0.50	32
135	1.962	0.981	0.017	4.504	0.44	36
133	1.943	0.972	0.017	4.546	0.48	33
131	1.927	0.963	0.017	4.585	0.44	35

$\zeta$  – correlation length in nm, determined with the Scherrer-equation

**Figure S10.** a) SAXS patterns in the isotropic mesophase of **3/12** on cooling from 145 to 131 °C with numerical values in the table; below 131 °C the cubic phase is formed during exposure time; b) WAXS on cooling from 145–117 °C (steps of 2K).



$T/^\circ\text{C}$	$2\theta/^\circ$	$\theta/^\circ$	$\theta/\text{rad}$	$d/\text{nm}$	$\text{FWHM}/^\circ$	$\zeta/\text{nm}$
145	2.232	1.116	0.019	3.958	0.78	26
143	2.175	1.088	0.019	4.061	0.71	27
141	2.139	1.069	0.019	4.131	0.66	28
139	2.070	1.035	0.018	4.268	0.59	29
137	2.023	1.011	0.018	4.367	0.49	34
135	1.997	0.999	0.017	4.424	0.46	35
133	1.995	0.998	0.017	4.428	0.26	63

$\zeta$  – correlation length in nm, determined with the Scherrer-equation

**Figure S11.** a) SAXS patterns in the isotropic mesophases of **3/14** on cooling from 145 to 133 °C with numerical values in the table; b) WAXS on cooling from 145–121 °C (steps of 2K).

### 2.3.4 Crystalline mesophase

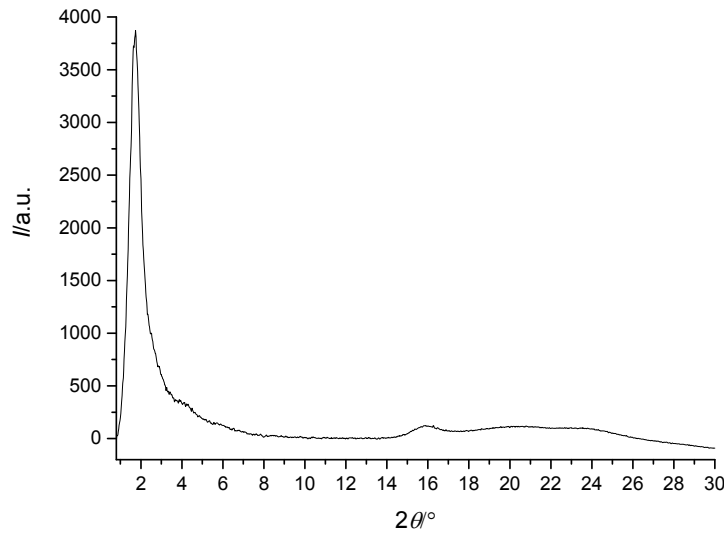


**Figure S12.** Full range XRD pattern of the crystalline isotropic mesophase ( $\text{Cr}_{\text{iso}}^{[*]}$ ) of **3/6** at 50 °C.

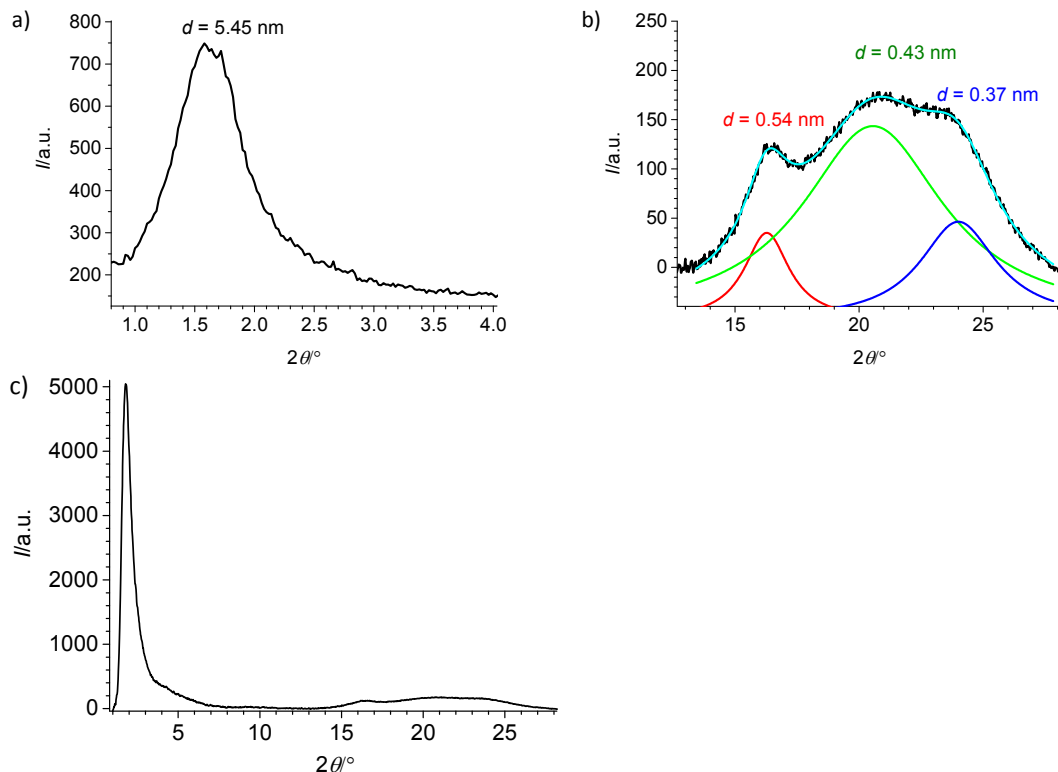


**Figure S13.** a) SAXS and b) WAXS pattern and c) full range XRD pattern of the conglomerate type chiral crystalline isotropic mesophase ( $\text{Cr}_{\text{iso}}^{[*]}$ ) of **3/10** at 25 °C.

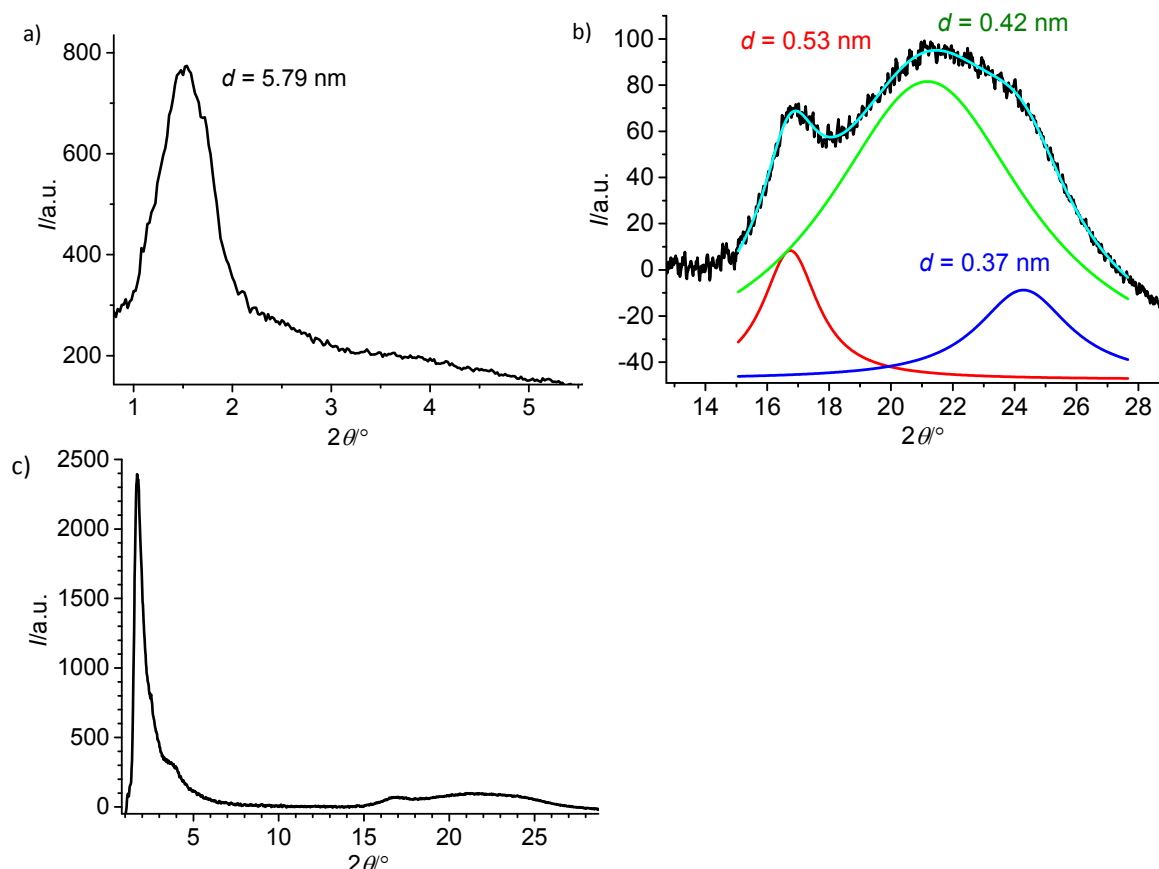


**Figure S14.** a) SAXS and b) WAXS pattern and c) full range XRD pattern of the achiral crystalline isotropic mesophase ( $\text{Cr}_{\text{iso}}$ ) of **3/12** at 25 °C.

## 2.4 Structural data

**Table S7.** Structural data of the cubic phases of the investigated compounds.<sup>a</sup>

Compd.	Phase	$a_{\text{cub}}/\text{nm}$	$V_{\text{cell}}/\text{nm}^3$	$V_{\text{mol}}/\text{nm}^3$	$n_{\text{cell}}^{\text{b}}$	$L_{\text{net}}^{\text{c}}/\text{nm}$	$n_{\text{strat}}^{\text{d}}$	$\Phi/{}^\circ \text{e}$
<b>3/2</b>	<i>Ia</i> 3 <i>d</i>	12.9	2147	1.59	1206	109.5	5.0	6.9
<b>3/4</b>	<i>I</i> 23	18.4	6230	1.64	3392	380.5	4.0	7.6
<b>3/6</b>	<i>I</i> 23	18.1	5930	1.69	3133	374.3	3.8	7.7
<b>3/10</b>	<i>I</i> 23	18.4	6230	1.79	3108	380.5	3.7	7.6
<b>3/12</b>	<i>Ia</i> 3 <i>d</i>	11.4	1482	1.84	719	96.7	3.3	7.9
<b>3/14</b>	<i>Ia</i> 3 <i>d</i>	11.3	1443	1.89	681	95.9	3.2	7.9
<b>3/16</b>	<i>Ia</i> 3 <i>d</i>	11.5	1521	1.94	700	97.6	3.2	7.8

<sup>a</sup> Abbreviations:  $n_{\text{cell}}$  number of molecules in a unit cell;  $V_{\text{cell}} = a_{\text{cub}}^3$  = volume of the unit cell;  $V_{\text{mol}}$  = molecular volume as calculated with the crystal volume increments of Immirizi<sup>S1</sup>;  $L_{\text{net}}$  = total network length per unit cell;  $n_{\text{strat}}$  = number of molecules organized side by side in each 0.45 nm high stratum of the column segments;  $\Phi$  = twist angle between adjacent molecules in the networks of the *Ia*3*d*- phases; <sup>b</sup>calculated according to 0.893  $V_{\text{cell}}/V_{\text{mol}}$ , where the factor 0.893 is a correction for the different packing density in the crystalline and the LC state; <sup>c</sup>  $L_{\text{net}}$  = total network length, calculated as  $L_{\text{net}} = 20.68 a_{123}$ ;  $L_{\text{net}} = 8.485 a_{\text{Ia3d}}$ ,<sup>S2</sup> <sup>d</sup>calculated according to  $n_{\text{cell}}/(L_{\text{net}}/0.45)$  for an assumed height of each stratum of  $h = 0.45 \text{ nm}$ ; <sup>e</sup>calculated according to:  $\Phi(\text{Ia3d}) = 70.5^\circ/[0.354 a_{\text{cub}}/0.45 \text{ nm}]$ ;  $\Phi(\text{I23}) = 90^\circ/[0.290 a_{\text{cub}}/0.45 \text{ nm}]$ ; though  $\Phi(\text{I23})$  refers to the inner and outer networks, the average twist in the middle network, consisting of shorter and longer segments is less than 1 % smaller.<sup>S2</sup>

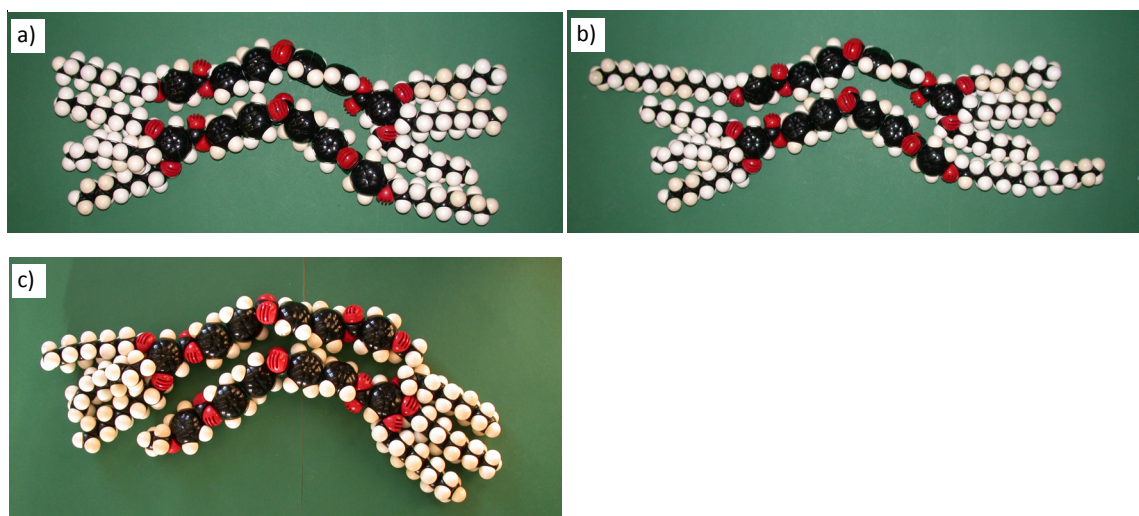


**Figure S15.** Space filling models of antiparallel pairs of compound a) **3/10** ( $L = 5.5 \text{ nm}$ ), b) **3/16** ( $L = 5.5 + 1.6 \text{ nm}$  for the overhangs of the longer chains) and c) **3/2** ( $L = 5.5 \text{ nm}$ ).

### 3. Additional Figures

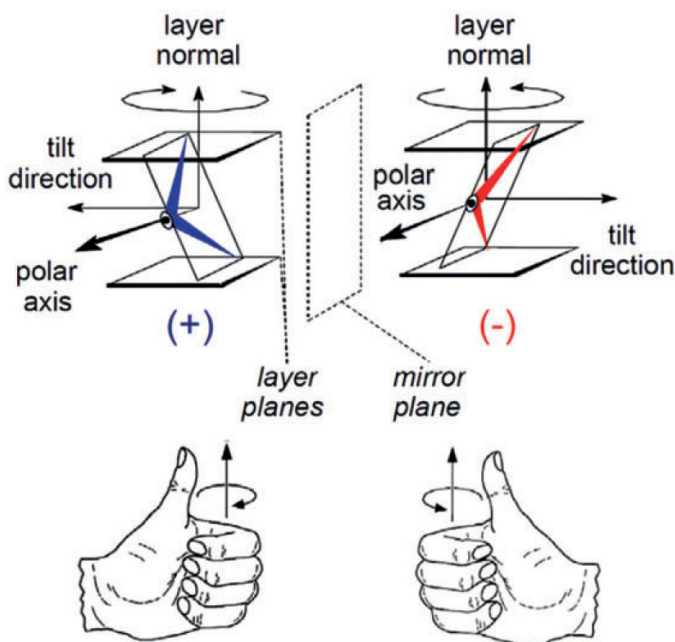
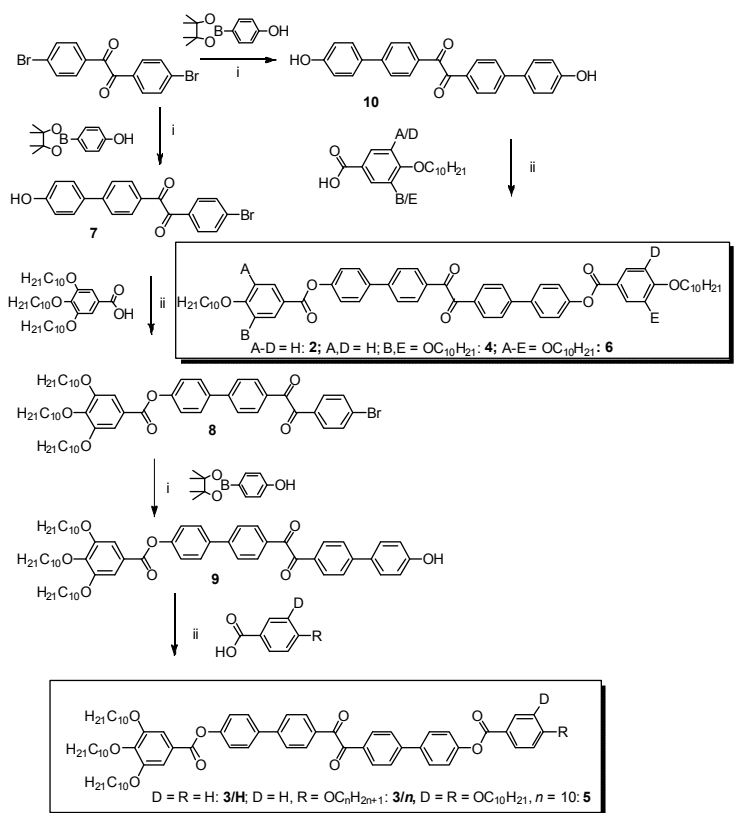


**Figure S16.** Layer chirality in the polar SmC phases of bent-core mesogens. The orthogonal combination of tilt and polar order leads to reduced  $C_{2v}$  symmetry and superstructural chirality of the layers (adapted from ref.<sup>S3</sup>); blue/red color indicates the chirality sense.

## 4. Synthesis and Analytical Data

### 4.1 General

Unless otherwise noted, all starting materials were purchased from commercial sources and were used without further purification. Column chromatography was performed with silica gel 60 (63-200 µm, Fluka). Determination of structures and purity of intermediates and products was obtained by NMR spectroscopy (VARIAN Gemini 2000 and Unity Inova 500, all spectra were recorded at 27 °C). Microanalyses were performed using a CARLO ERBA-CHNO 1102 elemental analyzer. The purity of all products was checked with thin layer chromatography (silicagel 60 F<sub>254</sub>, Merck). CHCl<sub>3</sub> and CHCl<sub>3</sub>/n-hexane mixtures were used as eluents and the spots were detected by UV radiation. 4-Hydroxyphenylboronic acid pinacol ester, 1,2-bis(4-bromophenyl)-1,2-ethanedione and 1,2-bis(4-hydroxyphenyl)-1,2-ethanedione were purchased from Sigma Aldrich and used as received. The 4-alkoxybenzoic acids were available from previous synthesis in our laboratory and have been synthesized by alkylation of ethyl 4-hydroxybenzoate followed by saponification.



**Scheme S1.** Synthesis of compounds **2/n-6/n**. Reagents and conditions: (i) THF, sat. NaHCO<sub>3</sub> solution, [Pd(PPh<sub>3</sub>)<sub>4</sub>], reflux; (ii) SOCl<sub>2</sub>, abs. pyridine, DCM, DMAP, 20 °C.

## 4.2 General procedures

**Procedure 1 (acylation):<sup>S 4</sup>** The appropriate carboxylic acid (1.25 equ) and SOCl<sub>2</sub> (2 ml/mmol) were refluxed for 30 minutes. SOCl<sub>2</sub> was removed under vacuum and dry pyridine (30 ml/mmol) and **9** (1.0 equ) were added and the resulting mixture was stirred at room temperature overnight. The solution was poured into ice/water and the resulting crude solid product was filtered off, dried and was purified by column chromatography and crystallization.

**Procedure 2 (Suzuki coupling):<sup>S 5</sup>** A mixture of the bromoarene (1 equ), 4-hydroxyphenylboronic acid pinacol ester (1.1 mmol) in THF (5 ml/mmol) and saturated NaHCO<sub>3</sub> solution (2.5 ml/mmol) was purged with argon for 15 minutes. A catalytic amount of [Pd(PPh<sub>3</sub>)<sub>4</sub>] was added and the solution was refluxed for 4 hours. After the reaction mixture reached room temperature (6 hrs), it was extracted twice with CHCl<sub>3</sub>. The organic layer was dried with Na<sub>2</sub>SO<sub>4</sub>, filtered and concentrated in vacuum. The crude product was purified by column chromatography and crystallization.

## 4.3 Intermediates

### 1-(4-Bromophenyl)-2-(4'-hydroxy-1,1'-biphenyl-4-yl)-1,2-ethanedione **7**

According to procedure **2** starting from 1,2-bis(4-bromophenyl)-1,2-ethanedione (7.1 g, 0.019 mol) and 4-hydroxyphenylboronic acid pinacol ester (4.7 g, 0.021 mol); purification by column chromatography (eluent: CHCl<sub>3</sub>/MeOH 9:1, v/v); yield 4.5 g (11.8 mmol, 61%); pale yellow solid; C<sub>20</sub>H<sub>13</sub>BrO<sub>3</sub>; *M* = 381.22 g/mol; m.p. 161 °C; <sup>1</sup>H NMR (400 MHz, CDCl<sub>3</sub>) δ

8.00 (d,  $^3J = 8.4$  Hz, 2H, Ar-H), 7.87 (d,  $^3J = 8.5$  Hz, 2H, Ar-H), 7.68 (d,  $^3J = 8.4$  Hz, 2H, Ar-H), 7.67 (d,  $^3J = 8.6$  Hz, 2H, Ar-H), 7.53 (d,  $^3J = 8.7$  Hz, 2H, Ar-H), 6.94 (d,  $^3J = 8.7$  Hz, 2H, Ar-H), 5.00 (s, 1H, OH).

### **1-[4'-(3,4,5-Tri-*n*-decyloxybenzoyloxy)-1,1'-biphenyl-4-yl]-2-(4-bromophenyl)-1,2-ethanedione 8**

According to procedure **1** starting from **7** (4.5 g, 0.012 mol) and 3,4,5-tri-*n*-decyloxybenzoic acid (8.0 g, 0.015 mol); purification by column chromatography (eluent: CHCl<sub>3</sub>) and crystallization from EtOH; yield 8.4 g (8.80 mmol, 75%); pale yellow solid; C<sub>57</sub>H<sub>77</sub>BrO<sub>7</sub>;  $M = 954.12$  g/mol; m.p. 81 °C; <sup>1</sup>H NMR (400 MHz, CDCl<sub>3</sub>) δ 8.05 (d,  $^3J = 8.3$  Hz, 2H, Ar-H), 7.88 (d,  $^3J = 8.5$  Hz, 2H, Ar-H), 7.74 (d,  $^3J = 8.4$  Hz, 2H, Ar-H), 7.68 (d,  $^3J = 8.5$  Hz, 4H, Ar-H), 7.42 (s, 2H, Ar-H), 7.32 (d,  $^3J = 8.6$  Hz, 2H, Ar-H), 4.09–4.03 (m, 6H, OCH<sub>2</sub>CH<sub>2</sub>), 1.89–1.80 (m, 4H, OCH<sub>2</sub>CH<sub>2</sub>), 1.79–1.73 (m, 2H, OCH<sub>2</sub>CH<sub>2</sub>), 1.53–1.45 (m, 6H, CH<sub>2</sub>), 1.41–1.21 (m, 36H, CH<sub>2</sub>), 0.91–0.83 (m, 9H, CH<sub>3</sub>).

### **1-[4'-(3,4,5-Tri-*n*-decyloxybenzoyloxy)-1,1'-biphenyl-4-yl]-2-(4'-hydroxy-1-1'-biphenyl-4-yl)-1,2-ethanedione 9**

According to procedure **2** starting from **9** (5.2 g, 5.45 mmol) and 4-hydroxyphenylboronic acid pinacol ester (1.2 g, 5.45 mmol); purification by column chromatography (eluent: CH<sub>2</sub>Cl<sub>2</sub>) and crystallization from EtOH; yield 3.5 g (3.62 mmol, 66%); pale yellow solid; C<sub>63</sub>H<sub>82</sub>O<sub>8</sub>;  $M = 967.32$  g/mol; m.p. 114 °C; <sup>1</sup>H NMR (400 MHz, CDCl<sub>3</sub>) δ 8.08 (d,  $^3J = 8.2$  Hz, 2H, Ar-H), 8.05 (d,  $^3J = 8.3$  Hz, 2H, Ar-H), 7.74 (d,  $^3J = 8.3$  Hz, 2H, Ar-H), 7.69 (d,  $^3J = 8.3$  Hz, 2H, Ar-H), 7.69 (d,  $^3J = 8.6$  Hz, 2H, Ar-H), 7.54 (d,  $^3J = 8.5$  Hz, 2H, Ar-H), 7.42 (s, 2H, Ar-H), 7.32 (d,  $^3J = 8.5$  Hz, 2H, Ar-H), 6.94 (d,  $^3J = 8.5$  Hz, 2H, Ar-H), 4.92 (s, 1H, OH), 4.10–4.03 (m, 6H, OCH<sub>2</sub>CH<sub>2</sub>), 1.88–1.79 (m, 4H, OCH<sub>2</sub>CH<sub>2</sub>), 1.79–1.73 (m, 2H, OCH<sub>2</sub>CH<sub>2</sub>), 1.52–1.44 (m, 6H, CH<sub>2</sub>), 1.41–1.21 (m, 36H, CH<sub>2</sub>), 0.92–0.84 (m, 9H, CH<sub>3</sub>).

### **1,2-Bis(4'-hydroxy-1,1'-biphenyl-4-yl)-1,2-ethanedione 10**

According to procedure **2** starting from 1,2-bis(4-bromophenyl)-1,2-ethanedione (400 mg, 1.09 mmol) and 4-hydroxyphenylboronic acid pinacol ester (530 mg, 2.39 mmol); purification by column chromatography (eluent: CHCl<sub>3</sub>/MeOH 9:1, v/v) and crystallization from MeOH/H<sub>2</sub>O; yield 210 mg (0.53 mmol, 49%); yellow solid; C<sub>26</sub>H<sub>18</sub>O<sub>4</sub>;  $M = 394.42$  g/mol; m.p. 274 °C; <sup>1</sup>H NMR (400 MHz, CD<sub>3</sub>OD) δ 7.98 (d,  $^3J = 8.5$  Hz, 4H, Ar-H), 7.78 (d,  $^3J = 8.5$  Hz, 4H, Ar-H), 7.58 (d,  $^3J = 8.7$  Hz, 4H, Ar-H), 6.89 (d,  $^3J = 8.7$  Hz, 4H, Ar-H).

## **4.4 Compounds 2 and 4-6**

### **1,2-Bis-[4'-(4-*n*-decyloxybenzoyloxy)-1,1'-biphenyl-4-yl]-1,2-ethanedione 2**

According to procedure **1** starting from **10** (57 mg, 0.145 mmol) and 4-*n*-decyloxybenzoic acid (101 mg, 0.361 mmol); purification by column chromatography (eluent: CHCl<sub>3</sub>) and crystallization from THF/MeOH; yield 104 mg (0.114 mmol, 78%); pale yellow solid; C<sub>60</sub>H<sub>66</sub>O<sub>8</sub>;  $M = 915.16$  g/mol; <sup>1</sup>H NMR (400 MHz, CDCl<sub>3</sub>) δ 8.16 (d,  $^3J = 9.0$  Hz, 4H, Ar-H), 8.09 (d,  $^3J = 8.6$  Hz, 4H, Ar-H), 7.75 (d,  $^3J = 8.7$  Hz, 4H, Ar-H), 7.69 (d,  $^3J = 8.8$  Hz, 4H, Ar-H), 7.33 (d,  $^3J = 8.8$  Hz, 4H, Ar-H), 6.98 (d,  $^3J = 9.0$  Hz, 4H, Ar-H), 4.05 (t,  $^3J = 6.6$  Hz, 4H, OCH<sub>2</sub>CH<sub>2</sub>), 1.87–1.79 (m, 4H, OCH<sub>2</sub>CH<sub>2</sub>), 1.51–1.44 (m, 4H, CH<sub>2</sub>), 1.42–1.23 (m, 24H, CH<sub>2</sub>), 0.92–0.86 (m, 6H, CH<sub>3</sub>); <sup>13</sup>C NMR (125 MHz, CDCl<sub>3</sub>) δ 194.0 (O=C-C=O), 164.8, 163.7 (C=O), 151.6, 146.8, 137.0, 132.3, 131.8, 130.6, 128.5, 127.6, 122.5, 121.3, 114.3 (Ar-C), 68.4 (OCH<sub>2</sub>), 31.9, 29.7, 29.5, 29.5, 29.3, 29.3, 29.1, 26.0, 22.7 (CH<sub>2</sub>), 14.1 (CH<sub>3</sub>); elemental analysis: calc for C<sub>60</sub>H<sub>66</sub>O<sub>8</sub>: C 78.74%, H 7.27%; found: C 78.80%, H 7.35%.

### **1,2-Bis-[4'-(3,4-di-*n*-decyloxybenzoyloxy)-1,1'-biphenyl-4-yl]-1,2-ethanedione 4**

According to procedure **1** starting from **10** (50 mg, 0.127 mmol) and 3,4-di-*n*-decyloxybenzoic acid (138 mg, 0.317 mmol); purification by column chromatography (eluent: CHCl<sub>3</sub>) and crystallization from THF/MeOH; yield 136 mg (0.111 mmol, 87%); pale yellow solid, C<sub>80</sub>H<sub>106</sub>O<sub>10</sub>; *M* = 1227.69 g/mol; <sup>1</sup>H NMR (500 MHz, CDCl<sub>3</sub>) δ 8.09 (d, <sup>3</sup>J = 8.4 Hz, 4H, Ar-H), 7.83 (dd, <sup>3</sup>J = 8.4 Hz, <sup>4</sup>J = 1.9 Hz, 2H, Ar-H), 7.75 (d, <sup>3</sup>J = 8.4 Hz, 4H, Ar-H), 7.70–7.66 (m, 6H, Ar-H), 7.32 (d, <sup>3</sup>J = 8.6 Hz, 4H, Ar-H), 6.94 (d, <sup>3</sup>J = 8.6 Hz, 2H, Ar-H), 4.11–4.05 (m, 8H, OCH<sub>2</sub>CH<sub>2</sub>), 1.90–1.81 (m, 8H, OCH<sub>2</sub>CH<sub>2</sub>), 1.51–1.45 (m, 8H, CH<sub>2</sub>), 1.41–1.21 (m, 48H, CH<sub>2</sub>), 0.91–0.85 (m, 12H, CH<sub>3</sub>); <sup>13</sup>C NMR (125 MHz, CDCl<sub>3</sub>) δ 194.0 (O=C-C=O), 164.9 (C=O), 154.0, 151.6, 148.7, 146.8, 137.0, 131.8, 130.6, 128.4, 127.6, 124.5, 122.5, 121.3, 114.7, 112.0 (Ar-C), 69.4, 69.1 (OCH<sub>2</sub>), 31.9, 29.6, 29.6, 29.5, 29.4, 29.4, 29.3, 29.2, 29.0, 26.0, 25.9, 22.7 (CH<sub>2</sub>), 14.1 (CH<sub>3</sub>); elemental analysis: calc for C<sub>80</sub>H<sub>106</sub>O<sub>10</sub>: C 78.27%, H 8.70%; found: C 78.16%, H 8.51%.

### **1-[4'-(3,4,5-Tri-*n*-decyloxybenzoyloxy)-1,1'-biphenyl-4-yl]-2-[4'-(3,4-di-*n*-decyloxybenzoyloxy)-1,1'-biphenyl-4-yl]-1,2-ethanedione 5**

According to procedure **1** starting from **9** (96 mg, 0.099 mmol) and 3,4-di-*n*-decyloxybenzoic acid (54 mg, 0.124 mmol); purification by column chromatography (eluent: CHCl<sub>3</sub>) and crystallization from THF/MeOH; yield 81 mg (0.059 mmol, 59%); pale yellow solid; C<sub>90</sub>H<sub>126</sub>O<sub>11</sub>; *M* = 1383.96 g/mol; <sup>1</sup>H NMR (500 MHz, CDCl<sub>3</sub>) δ 8.11 (d, <sup>3</sup>J = 7.6 Hz, 4H, Ar-H), 7.85 (dd, <sup>3</sup>J = 8.4 Hz, <sup>4</sup>J = 2.0 Hz, 1H, Ar-H), 7.77 (d, <sup>3</sup>J = 8.4 Hz, 4H, Ar-H), 7.73–7.68 (m, 5H, Ar-H), 7.44 (s, 2H, Ar-H), 7.34 (d, <sup>3</sup>J = 8.6 Hz, 2H, Ar-H), 7.33 (d, <sup>3</sup>J = 8.7 Hz, 2H, Ar-H), 6.96 (d, <sup>3</sup>J = 8.6 Hz, 1H, Ar-H), 4.13–4.04 (m, 10H, OCH<sub>2</sub>CH<sub>2</sub>), 1.92–1.81 (m, 8H, OCH<sub>2</sub>CH<sub>2</sub>), 1.81–1.74 (m, 2H, OCH<sub>2</sub>CH<sub>2</sub>), 1.55–1.46 (m, 10H, CH<sub>2</sub>), 1.42–1.22 (m, 60H, CH<sub>2</sub>), 0.93–0.86 (m, 15H, CH<sub>3</sub>); <sup>13</sup>C NMR (125 MHz, CDCl<sub>3</sub>) δ 194.0 (O=C-C=O), 164.9 (C=O), 154.0, 153.0, 151.7, 151.6, 148.7, 146.8, 146.7, 143.2, 137.2, 137.0, 131.8, 131.8, 130.6, 128.5, 128.5, 127.6, 124.5, 123.6, 122.5, 122.5, 121.3, 114.7, 112.0, 108.7 (Ar-C), 73.6, 69.4, 69.3, 69.1 (OCH<sub>2</sub>), 31.9, 31.9, 30.4, 29.7, 29.7, 29.6, 29.6, 29.6, 29.6, 29.4, 29.4, 29.3, 29.3, 29.2, 29.1, 26.1, 26.1, 26.0, 26.0, 22.7, 22.7 (CH<sub>2</sub>), 14.1 (CH<sub>3</sub>); elemental analysis: calc for C<sub>90</sub>H<sub>126</sub>O<sub>11</sub>: C 78.11%, H 9.18%; found: C 78.04%, H 9.08%.

### **1,2-Bis-[4'-(3,4,5-tri-*n*-decyloxybenzoyloxy)-1,1'-biphenyl-4-yl]-1,2-ethanedione 6**

According to procedure **1** starting from **10** (50 mg, 0.127 mmol) and 3,4,5-tri-*n*-decyloxybenzoic acid (187 mg, 0.317 mmol); purification by column chromatography (eluent: CHCl<sub>3</sub>/n-Hexan 4:1, v/v) and crystallization from THF/MeOH; yield 112 mg (0.073 mmol, 57%); pale yellow solid; C<sub>100</sub>H<sub>146</sub>O<sub>12</sub>; *M* = 1540.22 g/mol; <sup>1</sup>H NMR (400 MHz, CDCl<sub>3</sub>) δ 8.10 (d, <sup>3</sup>J = 8.5 Hz, 4H, Ar-H), 7.76 (d, <sup>3</sup>J = 8.5 Hz, 4H, Ar-H), 7.69 (d, <sup>3</sup>J = 8.7 Hz, 4H, Ar-H), 7.42 (s, 4H, Ar-H), 7.32 (d, <sup>3</sup>J = 8.6 Hz, 4H, Ar-H), 4.11–4.02 (m, 12H, OCH<sub>2</sub>CH<sub>2</sub>), 1.88–1.80 (m, 8H, OCH<sub>2</sub>CH<sub>2</sub>), 1.79–1.72 (m, 4H, OCH<sub>2</sub>CH<sub>2</sub>), 1.52–1.44 (m, 12H, CH<sub>2</sub>), 1.41–1.22 (m, 72H, CH<sub>2</sub>), 0.92–0.85 (m, 18H, CH<sub>3</sub>); <sup>13</sup>C NMR (125 MHz, CDCl<sub>3</sub>) δ 193.9 (O=C-C=O), 164.9 (C=O), 153.0, 151.5, 146.7, 143.2, 137.2, 131.8, 130.6, 128.5, 127.6, 123.6, 122.5, 108.7 (Ar-C), 73.6, 69.3 (OCH<sub>2</sub>), 31.9, 31.9, 30.3, 29.7, 29.7, 29.6, 29.6, 29.6, 29.4, 29.3, 29.3, 26.1, 26.0, 22.7, 22.7 (CH<sub>2</sub>), 14.1 (CH<sub>3</sub>); elemental analysis: calc for C<sub>100</sub>H<sub>146</sub>O<sub>12</sub>: C 77.98%, H 9.55%; found: C 77.68%, H 9.51%.

## **4.5 Compounds 3/H and 3/n**

### **1-[4'-(3,4,5-Tri-*n*-decyloxybenzoyloxy)-1,1'-biphenyl-4-yl]-2-(4'-benzoyloxy-1,1'-biphenyl-4-yl)-1,2-ethanedione 3/H**

According to procedure **1** starting from **9** (98 mg, 0.101 mmol) and benzoic acid (16 mg, 0.127 mmol); purification by column chromatography (eluent: CHCl<sub>3</sub>/n-Hexan 4:1, v/v) and

crystallization from THF/MeOH; yield 76 mg (0.071 mmol, 70%); pale yellow solid; C<sub>70</sub>H<sub>86</sub>O<sub>9</sub>; M = 1071.43 g/mol; <sup>1</sup>H NMR (400 MHz, CDCl<sub>3</sub>) δ 8.23 (dd, <sup>3</sup>J = 8.3 Hz, <sup>4</sup>J = 1.2 Hz, 2H, Ar-H), 8.10 (d, <sup>3</sup>J = 8.4 Hz, 4H, Ar-H), 7.76 (d, <sup>3</sup>J = 8.5 Hz, 4H, Ar-H), 7.70 (d, <sup>3</sup>J = 8.7 Hz, 2H, Ar-H), 7.69 (d, <sup>3</sup>J = 8.7 Hz, 2H, Ar-H), 7.67–7.63 (m, 1H, Ar-H), 7.57–7.51 (m, 2H, Ar-H), 7.42 (s, 2H, Ar-H), 7.35 (d, <sup>3</sup>J = 8.7 Hz, 2H, Ar-H), 7.32 (d, <sup>3</sup>J = 8.7 Hz, 2H, Ar-H), 4.10–4.03 (m, 6H, OCH<sub>2</sub>CH<sub>2</sub>), 1.88–1.79 (m, 4H, OCH<sub>2</sub>CH<sub>2</sub>), 1.79–1.72 (m, 2H, OCH<sub>2</sub>CH<sub>2</sub>), 1.52–1.44 (m, 6H, CH<sub>2</sub>), 1.41–1.22 (m, 36H, CH<sub>2</sub>), 0.92–0.85 (m, 9H, CH<sub>3</sub>); <sup>13</sup>C NMR (125 MHz, CDCl<sub>3</sub>) δ 193.9 (O=C-C=O), 165.0, 164.8 (C=O), 152.9, 151.5, 151.4, 146.6, 143.1, 137.2, 137.1, 133.7, 131.7, 130.5, 130.1, 129.2, 128.5, 128.4, 128.4, 127.5, 127.5, 123.5, 122.4, 122.3, 108.6 (Ar-C), 73.5, 69.2 (OCH<sub>2</sub>), 31.8, 31.8, 30.2, 29.6, 29.6, 29.5, 29.5, 29.5, 29.3, 29.2, 29.2, 26.0, 26.0, 22.6, 22.6 (CH<sub>2</sub>), 14.0 (CH<sub>3</sub>); elemental analysis: calc for C<sub>70</sub>H<sub>86</sub>O<sub>9</sub>: C 78.47%, H 8.09%; found: C 78.18%, H 7.97%.

### **1-[4'-(3,4,5-Tri-*n*-decyloxybenzoyloxy)-1,1'-biphenyl-4-yl]-2-[4'-(4-methoxybenzoyloxy)-1,1'-biphenyl-4-yl]-1,2-ethanedione 3/1**

According to procedure **1** starting from **9** (106 mg, 0.110 mmol) and 4-methoxybenzoic acid (21 mg, 0.137 mmol); purification by column chromatography (eluent: CHCl<sub>3</sub>) and crystallization from THF/MeOH; yield 60 mg (0.054 mmol, 50%); pale yellow solid; C<sub>71</sub>H<sub>88</sub>O<sub>10</sub>; M = 1101.45 g/mol; <sup>1</sup>H NMR (500 MHz, CDCl<sub>3</sub>) δ 8.19 (d, <sup>3</sup>J = 9.0 Hz, 2H, Ar-H), 8.11 (d, <sup>3</sup>J = 8.5 Hz, 2H, Ar-H), 8.11 (d, <sup>3</sup>J = 8.3 Hz, 2H, Ar-H), 7.77 (d, <sup>3</sup>J = 8.6 Hz, 2H, Ar-H), 7.77 (d, <sup>3</sup>J = 8.2 Hz, 2H, Ar-H), 7.71 (d, <sup>3</sup>J = 8.8 Hz, 2H, Ar-H), 7.70 (d, <sup>3</sup>J = 8.7 Hz, 2H, Ar-H), 7.44 (s, 2H, Ar-H), 7.35 (d, <sup>3</sup>J = 8.6 Hz, 2H, Ar-H), 7.33 (d, <sup>3</sup>J = 8.6 Hz, 2H, Ar-H), 7.02 (d, <sup>3</sup>J = 9.0 Hz, 2H, Ar-H), 4.10–4.05 (m, 6H, OCH<sub>2</sub>CH<sub>2</sub>), 3.92 (s, 3H, OCH<sub>3</sub>), 1.89–1.82 (m, 4H, OCH<sub>2</sub>CH<sub>2</sub>), 1.81–1.75 (m, 2H, OCH<sub>2</sub>CH<sub>2</sub>), 1.54–1.46 (m, 6H, CH<sub>2</sub>), 1.42–1.23 (m, 36H, CH<sub>2</sub>), 0.93–0.85 (m, 9H, CH<sub>3</sub>); <sup>13</sup>C NMR (100 MHz, CDCl<sub>3</sub>) δ 194.0 (O=C-C=O), 164.9, 164.8 (C=O), 164.0, 153.0, 151.6, 151.5, 146.8, 146.7, 143.2, 137.2, 137.0, 132.4, 131.8, 131.8, 130.6, 128.5, 128.5, 127.6, 123.6, 122.5, 122.5, 121.6, 113.9, 108.7 (Ar-C), 73.6, 69.3 (OCH<sub>2</sub>), 55.5 (OCH<sub>3</sub>), 31.9, 31.9, 30.3, 29.7, 29.7, 29.6, 29.6, 29.5, 29.4, 29.3, 29.3, 26.1, 26.0, 22.7, 22.7 (CH<sub>2</sub>), 14.1 (CH<sub>3</sub>); elemental analysis: calc for C<sub>71</sub>H<sub>88</sub>O<sub>10</sub>: C 77.42%, H 8.05%; found: C 77.17%, H 7.95%.

### **1-[4'-(3,4,5-Tri-*n*-decyloxybenzoyloxy)-1,1'-biphenyl-4-yl]-2-[4'-(4-ethoxybenzoyloxy)-1,1'-biphenyl-4-yl]-1,2-ethanedione 3/2**

According to procedure **1** starting from **9** (110 mg, 0.114 mmol) and 4-ethoxybenzoic acid (24 mg, 0.142 mmol); purification by column chromatography (eluent: CHCl<sub>3</sub>) and crystallization from THF/MeOH; yield 61 mg (0.055 mmol, 48%); pale yellow solid; C<sub>72</sub>H<sub>90</sub>O<sub>10</sub>; M = 1115.48 g/mol; <sup>1</sup>H NMR (400 MHz, CDCl<sub>3</sub>) δ 8.16 (d, <sup>3</sup>J = 8.9 Hz, 2H, Ar-H), 8.11–8.07 (m, 4H, Ar-H), 7.78–7.73 (m, 4H, Ar-H), 7.69 (d, <sup>3</sup>J = 8.8 Hz, 2H, Ar-H), 7.69 (d, <sup>3</sup>J = 8.7 Hz, 2H, Ar-H), 7.42 (s, 2H, Ar-H), 7.33 (d, <sup>3</sup>J = 8.6 Hz, 2H, Ar-H), 7.32 (d, <sup>3</sup>J = 8.6 Hz, 2H, Ar-H), 6.99 (d, <sup>3</sup>J = 8.9 Hz, 2H, Ar-H), 4.14 (q, <sup>3</sup>J = 7.0 Hz, 2H, OCH<sub>2</sub>CH<sub>3</sub>), 4.10–4.03 (m, 6H, OCH<sub>2</sub>CH<sub>2</sub>), 1.89–1.80 (m, 4H, OCH<sub>2</sub>CH<sub>2</sub>), 1.80–1.72 (m, 2H, OCH<sub>2</sub>CH<sub>2</sub>), 1.53–1.44 (m, 6H, CH<sub>2</sub>), 1.47 (t, <sup>3</sup>J = 7.0 Hz, 3H, OCH<sub>2</sub>CH<sub>3</sub>), 1.41–1.22 (m, 36H, CH<sub>2</sub>), 0.92–0.84 (m, 9H, CH<sub>3</sub>); <sup>13</sup>C NMR (125 MHz, CDCl<sub>3</sub>) δ 194.0 (O=C-C=O), 164.9, 164.8 (C=O), 163.5, 153.0, 151.6, 151.6, 146.8, 146.7, 143.2, 137.2, 137.0, 132.4, 131.8, 131.8, 130.6, 128.5, 128.5, 127.6, 123.6, 122.5, 122.5, 121.3, 114.3, 108.7 (Ar-C), 73.6, 69.3, 63.8 (OCH<sub>2</sub>), 31.9, 31.9, 30.4, 29.7, 29.7, 29.6, 29.6, 29.4, 29.3, 29.3, 26.1, 26.1, 22.7, 22.7 (CH<sub>2</sub>), 14.7, 14.1 (CH<sub>3</sub>); elemental analysis: calc for C<sub>72</sub>H<sub>90</sub>O<sub>10</sub>: C 77.52%, H 8.13%; found: C 77.28%, H 7.91%.

### **1-[4'-(3,4,5-Tri-*n*-decyloxybenzoyloxy)-1,1'-biphenyl-4-yl]-2-[4'-(4-*n*-butyloxybenzoyloxy)-1,1'-biphenyl-4-yl]-1,2-ethanedione 3/4**

According to procedure **1** starting from **9** (108 mg, 0.112 mmol) and 4-*n*-butyloxy-benzoic acid (27 mg, 0.140 mmol); purification by column chromatography (eluent: CHCl<sub>3</sub>) and crystallization from THF/MeOH; yield 99 mg (0.087 mmol, 77%); pale yellow solid; C<sub>74</sub>H<sub>94</sub>O<sub>10</sub>; *M* = 1143.53 g/mol; <sup>1</sup>H NMR (400 MHz, CDCl<sub>3</sub>) δ 8.16 (d, <sup>3</sup>J = 8.9 Hz, 2H, Ar-H), 8.11–8.07 (m, 4H, Ar-H), 7.75 (d, <sup>3</sup>J = 8.2 Hz, 4H, Ar-H), 7.69 (d, <sup>3</sup>J = 8.8 Hz, 2H, Ar-H), 7.69 (d, <sup>3</sup>J = 8.8 Hz, 2H, Ar-H), 7.42 (s, 2H, Ar-H), 7.33 (d, <sup>3</sup>J = 8.6 Hz, 2H, Ar-H), 7.32 (d, <sup>3</sup>J = 8.7 Hz, 2H, Ar-H), 6.99 (d, <sup>3</sup>J = 9.0 Hz, 2H, Ar-H), 4.10–4.02 (m, 8H, OCH<sub>2</sub>CH<sub>2</sub>), 1.88–1.79 (m, 6H, OCH<sub>2</sub>CH<sub>2</sub>), 1.79–1.72 (m, 2H, OCH<sub>2</sub>CH<sub>2</sub>), 1.58–1.44 (m, 8H, CH<sub>2</sub>), 1.41–1.20 (m, 36H), 1.00 (t, <sup>3</sup>J = 7.4 Hz, 3H, CH<sub>3</sub>), 0.93–0.84 (m, 9H, CH<sub>3</sub>); <sup>13</sup>C NMR (100 MHz, CDCl<sub>3</sub>) δ 194.0 (O=C-C=O), 164.9, 164.8 (C=O), 163.7, 153.0, 151.6, 151.5, 146.8, 146.7, 143.2, 137.2, 137.0, 132.3, 131.8, 131.8, 130.6, 128.5, 128.5, 127.6, 123.6, 122.5, 122.4, 121.3, 114.3, 108.7 (Ar-C), 73.6, 69.3, 68.0 (OCH<sub>2</sub>), 31.9, 31.9, 31.1, 30.3, 29.7, 29.7, 29.6, 29.6, 29.5, 29.4, 29.3, 29.3, 26.1, 26.0, 22.7, 22.7, 19.2 (CH<sub>2</sub>), 14.1, 13.8 (CH<sub>3</sub>); elemental analysis: calc for C<sub>74</sub>H<sub>94</sub>O<sub>10</sub>: C 77.72%, H 8.29%; found: C 77.69%, H 8.01%.

### **1-[4'-(3,4,5-Tri-*n*-decyloxybenzoyloxy)-1,1'-biphenyl-4-yl]-2-[4'-(4-hexyloxybenzoyloxy)-1,1'-biphenyl-4-yl]-1,2-ethanedione 3/6**

According to procedure **1** starting from **9** (96 mg, 0.099 mmol) and 4-*n*-hexyloxy-benzoic acid (27 mg, 0.124 mmol); purification by column chromatography (eluent: CHCl<sub>3</sub>) and crystallization from THF/MeOH; yield 83 mg (0.071 mmol, 72%); pale yellow solid; C<sub>76</sub>H<sub>98</sub>O<sub>10</sub>; *M* = 1171.59 g/mol; <sup>1</sup>H NMR (500 MHz, CDCl<sub>3</sub>) δ 8.16 (d, <sup>3</sup>J = 8.9 Hz, 2H, Ar-H), 8.10 (d, <sup>3</sup>J = 8.5 Hz, 2H, Ar-H), 8.09 (d, <sup>3</sup>J = 8.5 Hz, 2H, Ar-H), 7.76 (d, <sup>3</sup>J = 8.5 Hz, 2H, Ar-H), 7.76 (d, <sup>3</sup>J = 8.6 Hz, 2H, Ar-H), 7.70 (d, <sup>3</sup>J = 8.7 Hz, 2H, Ar-H), 7.69 (d, <sup>3</sup>J = 8.7 Hz, 2H, Ar-H), 7.42 (s, 2H, Ar-H), 7.33 (d, <sup>3</sup>J = 8.6 Hz, 2H, Ar-H), 7.32 (d, <sup>3</sup>J = 8.6 Hz, 2H), 6.99 (d, <sup>3</sup>J = 9.0 Hz, 2H, Ar-H), 4.09–4.04 (m, 8H, OCH<sub>2</sub>CH<sub>2</sub>), 1.87–1.80 (m, 6H, OCH<sub>2</sub>CH<sub>2</sub>), 1.80–1.73 (m, 2H, OCH<sub>2</sub>CH<sub>2</sub>), 1.53–1.45 (m, 8H, CH<sub>2</sub>), 1.41–1.22 (m, 40H, CH<sub>2</sub>), 0.95–0.86 (m, 12H, CH<sub>3</sub>); <sup>13</sup>C NMR (125 MHz, CDCl<sub>3</sub>) δ 165.1, 164.9 (C=O), 153.0, 150.5, 144.5, 143.1, 142.3, 142.3, 136.8, 136.7, 131.8, 131.8, 130.2, 129.3, 126.7, 126.7, 126.6, 124.6, 124.0, 123.7, 122.3, 122.3, 108.6 (Ar-C), 73.6, 69.3 (OCH<sub>2</sub>), 31.9, 31.9, 30.3, 29.7, 29.7, 29.6, 29.6, 29.6, 29.4, 29.3, 29.3, 26.1, 26.0, 22.7, 22.7, 21.8 (CH<sub>2</sub>), 14.1 (CH<sub>3</sub>); elemental analysis: calc for C<sub>76</sub>H<sub>98</sub>O<sub>10</sub>: C 77.91%, H 8.43%; found: C 77.92%, H 8.40%.

### **1-[4'-(3,4,5-Tri-*n*-decyloxybenzoyloxy)-1,1'-biphenyl-4-yl]-2-[4'-(4-*n*-decyloxybenzoyloxy)-1,1'-biphenyl-4-yl]-1,2-ethanedione 3/10**

According to procedure **1** starting from **9** (94 mg, 0.097 mmol) and 4-*n*-decyloxy-benzoic acid (34 mg, 0.121 mmol); purification by column chromatography (eluent: CHCl<sub>3</sub>) and crystallization from THF/MeOH; yield 64 mg (0.052 mmol, 55%); pale yellow solid; C<sub>80</sub>H<sub>106</sub>O<sub>10</sub>; *M* = 1227.69 g/mol; <sup>1</sup>H NMR (400 MHz, CDCl<sub>3</sub>) δ 8.16 (d, <sup>3</sup>J = 8.7 Hz, 2H, Ar-H), 8.09 (d, <sup>3</sup>J = 8.2 Hz, 4H, Ar-H), 7.75 (d, <sup>3</sup>J = 8.1 Hz, 4H, Ar-H), 7.69 (d, <sup>3</sup>J = 8.7 Hz, 2H, Ar-H), 7.69 (d, <sup>3</sup>J = 8.7 Hz, 2H, Ar-H), 7.42 (s, 2H, Ar-H), 7.33 (d, <sup>3</sup>J = 8.5 Hz, 2H, Ar-H), 7.32 (d, <sup>3</sup>J = 8.6 Hz, 2H, Ar-H), 6.98 (d, <sup>3</sup>J = 8.8 Hz, 2H, Ar-H), 4.09–4.02 (m, 8H, OCH<sub>2</sub>CH<sub>2</sub>), 1.88–1.80 (m, 6H, OCH<sub>2</sub>CH<sub>2</sub>), 1.80–1.72 (m, 2H, OCH<sub>2</sub>CH<sub>2</sub>), 1.52–1.44 (m, 8H, CH<sub>2</sub>), 1.41–1.22 (m, 48H, CH<sub>2</sub>), 0.91–0.85 (m, 12H, CH<sub>3</sub>); <sup>13</sup>C NMR (125 MHz, CDCl<sub>3</sub>) δ 194.0 (O=C-C=O), 164.9, 164.8 (C=O), 163.7, 153.0, 151.6, 151.6, 146.8, 146.7, 143.2, 137.2, 137.0, 132.3, 131.8, 131.8, 130.6, 128.5, 128.5, 127.6, 123.6, 122.5, 122.5, 121.3, 114.4, 108.7 (Ar-C), 73.6, 69.3, 68.4 (OCH<sub>2</sub>), 31.9, 31.9, 31.9, 30.4, 29.7, 29.7, 29.6, 29.6, 29.6, 29.5, 29.4, 29.4, 29.3, 29.3, 29.1, 26.1, 26.1, 26.0, 22.7, 22.7 (CH<sub>2</sub>), 14.1 (CH<sub>3</sub>); elemental analysis: calc for C<sub>80</sub>H<sub>106</sub>O<sub>10</sub>: C 78.27%, H 8.70%; found: C 78.02%, H 8.64%.

### **1-[4'-(3,4,5-Tri-*n*-decyloxybenzoyloxy)-1,1'-biphenyl-4-yl]-2-[4'-(4-*n*-dodecyloxybenzoyloxy)-1,1'-biphenyl-4-yl]-1,2-ethanedione 3/12**

According to procedure **1** starting from **9** (106 mg, 0.110 mmol) and 4-*n*-dodecyloxybenzoic acid (42 mg, 0.137 mmol); purification by column chromatography (eluent: CHCl<sub>3</sub>) and crystallization from THF/MeOH; yield 88 mg (0.070 mmol, 64%); pale yellow solid; C<sub>82</sub>H<sub>110</sub>O<sub>10</sub>; *M* = 1255.74 g/mol; <sup>1</sup>H NMR (400 MHz, CDCl<sub>3</sub>) δ 8.17 (d, <sup>3</sup>J = 8.9 Hz, 2H, Ar-H), 8.10 (d, <sup>3</sup>J = 8.2 Hz, 2H, Ar-H), 8.10 (d, <sup>3</sup>J = 8.4 Hz, 2H, Ar-H), 7.78–7.74 (m, 4H, Ar-H), 7.70 (d, <sup>3</sup>J = 8.7 Hz, 2H, Ar-H), 7.69 (d, <sup>3</sup>J = 8.7 Hz, 2H, Ar-H), 7.43 (s, 2H, Ar-H), 7.34 (d, <sup>3</sup>J = 8.6 Hz, 2H, Ar-H), 7.33 (d, <sup>3</sup>J = 8.6 Hz, 2H, Ar-H), 6.99 (d, <sup>3</sup>J = 8.9 Hz, 2H, Ar-H), 4.11–4.03 (m, 8H, OCH<sub>2</sub>CH<sub>2</sub>), 1.89–1.80 (m, 6H, OCH<sub>2</sub>CH<sub>2</sub>), 1.80–1.73 (m, 2H, OCH<sub>2</sub>CH<sub>2</sub>), 1.54–1.44 (m, 8H, CH<sub>2</sub>), 1.42–1.22 (m, 52H, CH<sub>2</sub>), 0.94–0.86 (m, 12H, CH<sub>3</sub>); <sup>13</sup>C NMR (100 MHz, CDCl<sub>3</sub>) δ 194.0 (O=C-C=O), 164.9, 164.8 (C=O), 163.7, 153.0, 151.6, 151.5, 146.8, 146.7, 143.2, 137.2, 137.0, 132.3, 131.8, 131.8, 130.6, 128.5, 128.5, 127.6, 123.6, 122.5, 122.5, 121.3, 114.4, 108.7 (Ar-C), 73.6, 69.3, 68.4 (OCH<sub>2</sub>), 31.9, 31.9, 30.3, 29.7, 29.7, 29.6, 29.6, 29.6, 29.5, 29.4, 29.3, 29.3, 29.1, 26.1, 26.1, 26.0, 22.7, 22.7 (CH<sub>2</sub>), 14.1, 14.1 (CH<sub>3</sub>); elemental analysis: calc for C<sub>82</sub>H<sub>110</sub>O<sub>10</sub>: C 78.43%, H 8.83%; found: C 78.25%, H 8.77%.

### **1-[4'-(3,4,5-Tri-*n*-decyloxybenzoyloxy)-1,1'-biphenyl-4-yl]-2-[4'-(4-*n*-tetradecyloxybenzoyloxy)-1,1'-biphenyl-4-yl]-1,2-ethanedione 3/14**

According to procedure **1** starting from **9** (108 mg, 0.112 mmol) and 4-*n*-tetradecyloxybenzoic acid (47 mg, 0.140 mmol); purification by column chromatography (eluent: CHCl<sub>3</sub>) and crystallization from THF/MeOH; yield 75 mg (0.058 mmol, 52%); pale yellow solid; C<sub>84</sub>H<sub>114</sub>O<sub>10</sub>; *M* = 1283.80 g/mol; <sup>1</sup>H NMR (400 MHz, CDCl<sub>3</sub>) δ 8.17 (d, <sup>3</sup>J = 8.9 Hz, 2H, Ar-H), 8.10 (d, <sup>3</sup>J = 8.3 Hz, 2H, Ar-H), 8.10 (d, <sup>3</sup>J = 8.4 Hz, 2H, Ar-H), 7.79–7.74 (m, 4H, Ar-H), 7.70 (d, <sup>3</sup>J = 8.7 Hz, 2H, Ar-H), 7.69 (d, <sup>3</sup>J = 8.7 Hz, 2H, Ar-H), 7.43 (s, 2H, Ar-H), 7.34 (d, <sup>3</sup>J = 8.6 Hz, 2H, Ar-H), 7.33 (d, <sup>3</sup>J = 8.6 Hz, 2H, Ar-H), 6.99 (d, <sup>3</sup>J = 8.9 Hz, 2H, Ar-H), 4.11–4.02 (m, 8H, OCH<sub>2</sub>CH<sub>2</sub>), 1.89–1.80 (m, 6H, OCH<sub>2</sub>CH<sub>2</sub>), 1.80–1.73 (m, 2H, OCH<sub>2</sub>CH<sub>2</sub>), 1.53–1.44 (m, 8H, CH<sub>2</sub>), 1.42–1.22 (m, 56H, CH<sub>2</sub>), 0.93–0.86 (m, 12H, CH<sub>3</sub>); <sup>13</sup>C NMR (100 MHz, CDCl<sub>3</sub>) δ 194.0 (O=C-C=O), 164.9, 164.8 (C=O), 163.7, 153.0, 151.6, 151.5, 146.8, 146.7, 143.2, 137.2, 137.0, 132.3, 131.8, 131.8, 130.6, 128.5, 128.5, 127.6, 123.6, 122.5, 122.5, 121.3, 114.4, 108.7 (Ar-C), 73.6, 69.3, 68.4 (OCH<sub>2</sub>), 31.9, 31.9, 31.9, 30.3, 29.7, 29.7, 29.6, 29.6, 29.6, 29.4, 29.3, 29.3, 29.1, 26.1, 26.1, 26.0, 22.7 (CH<sub>2</sub>), 14.1, 14.1 (CH<sub>3</sub>); elemental analysis: calc for C<sub>84</sub>H<sub>114</sub>O<sub>10</sub>: C 78.59%, H 8.95%; found: C 78.59%, H 8.85%.

### **1-[4'-(3,4,5-Tri-*n*-decyloxybenzoyloxy)-1,1'-biphenyl-4-yl]-2-[4'-(4-*n*-hexadecyloxybenzoyloxy)-1,1'-biphenyl-4-yl]-1,2-ethanedione 3/16**

According to procedure **1** starting from **9** (91 mg, 0.094 mmol) and 4-*n*-hexadecyloxybenzoic acid (43 mg, 0.118 mmol); purification by column chromatography (eluent: CHCl<sub>3</sub>) and crystallization from THF/MeOH; yield 71 mg (0.054 mmol, 58%); pale yellow solid; C<sub>86</sub>H<sub>118</sub>O<sub>10</sub>; *M* = 1311.85 g/mol; <sup>1</sup>H NMR (400 MHz, CDCl<sub>3</sub>) δ 8.16 (d, <sup>3</sup>J = 8.9 Hz, 2H, Ar-H), 8.09 (d, <sup>3</sup>J = 8.6 Hz, 2H), 8.09 (d, <sup>3</sup>J = 8.3 Hz, 2H, Ar-H), 7.75 (d, <sup>3</sup>J = 8.7 Hz, 2H, Ar-H), 7.75 (d, <sup>3</sup>J = 8.2 Hz, 2H, Ar-H), 7.69 (d, <sup>3</sup>J = 8.8 Hz, 2H, Ar-H), 7.69 (d, <sup>3</sup>J = 8.7 Hz, 2H, Ar-H), 7.42 (s, 2H, Ar-H), 7.33 (d, <sup>3</sup>J = 8.6 Hz, 2H, Ar-H), 7.32 (d, <sup>3</sup>J = 8.6 Hz, 2H, Ar-H), 6.98 (d, <sup>3</sup>J = 8.9 Hz, 2H, Ar-H), 4.09–4.03 (m, 8H, OCH<sub>2</sub>CH<sub>2</sub>), 1.88–1.80 (m, 6H, OCH<sub>2</sub>CH<sub>2</sub>), 1.79–1.72 (m, 2H, OCH<sub>2</sub>CH<sub>2</sub>), 1.52–1.43 (m, 8H, CH<sub>2</sub>), 1.41–1.21 (m, 60H, CH<sub>2</sub>), 0.91–0.85 (m, 12H, CH<sub>3</sub>); <sup>13</sup>C NMR (126 MHz, CDCl<sub>3</sub>) δ 194.0 (O=C-C=O), 164.9, 164.8 (C=O), 163.7, 153.0, 151.6, 151.6, 146.8, 146.7, 143.2, 137.2, 137.0, 132.3, 131.8, 131.8, 130.6, 128.5, 128.5, 127.6, 123.6, 122.5, 122.5, 121.3, 114.4, 108.7 (Ar-C), 73.6, 69.3, 68.4 (OCH<sub>2</sub>), 31.9, 31.9, 31.9, 30.4, 29.7, 29.7, 29.6, 29.6, 29.6, 29.5, 29.4, 29.4, 29.3, 29.3, 29.1, 26.1, 26.1, 26.0, 22.7, 22.7 (CH<sub>2</sub>), 14.1, 14.1 (CH<sub>3</sub>); elemental analysis: calc for C<sub>86</sub>H<sub>118</sub>O<sub>10</sub>: C 78.74%, H 9.07%; found: C 78.81%, H 8.89%.

## 4.6 Representative NMR spectra

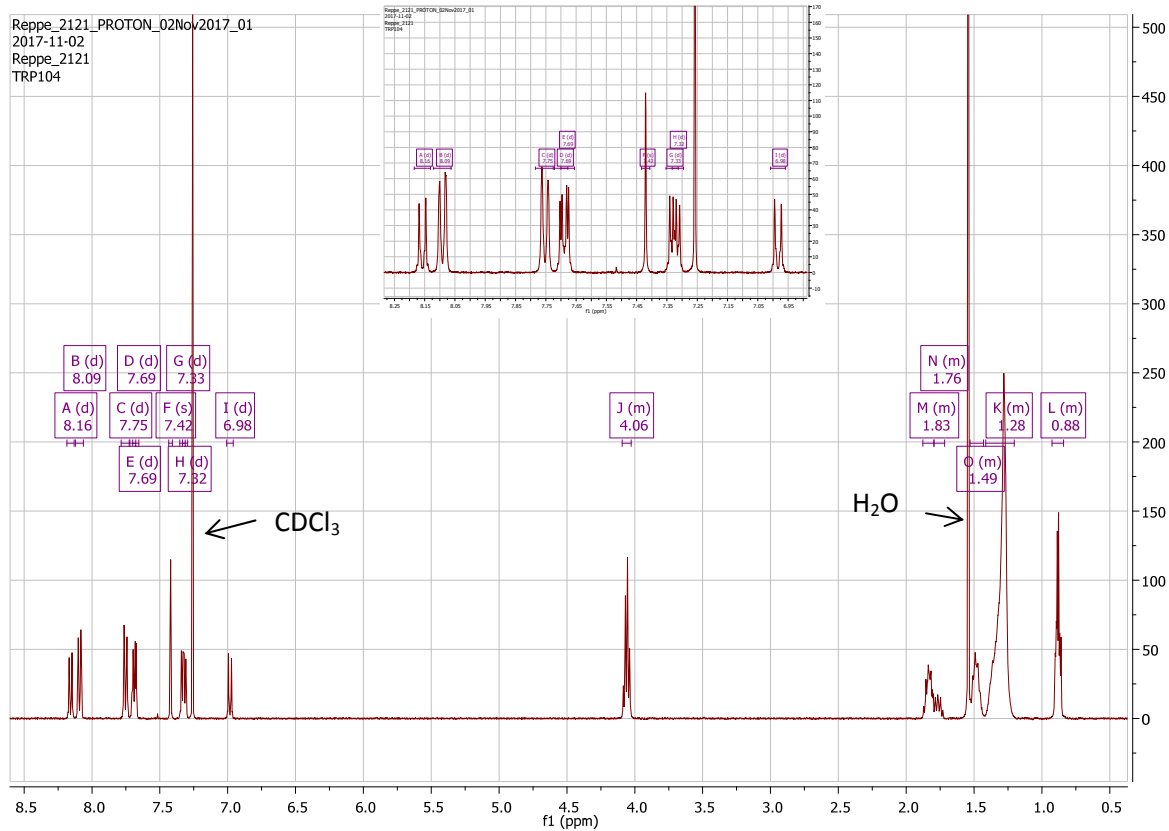


Figure S17.  $^1\text{H}$ -NMR spectrum of 3/10 (400 MHz,  $\text{CDCl}_3$ ).

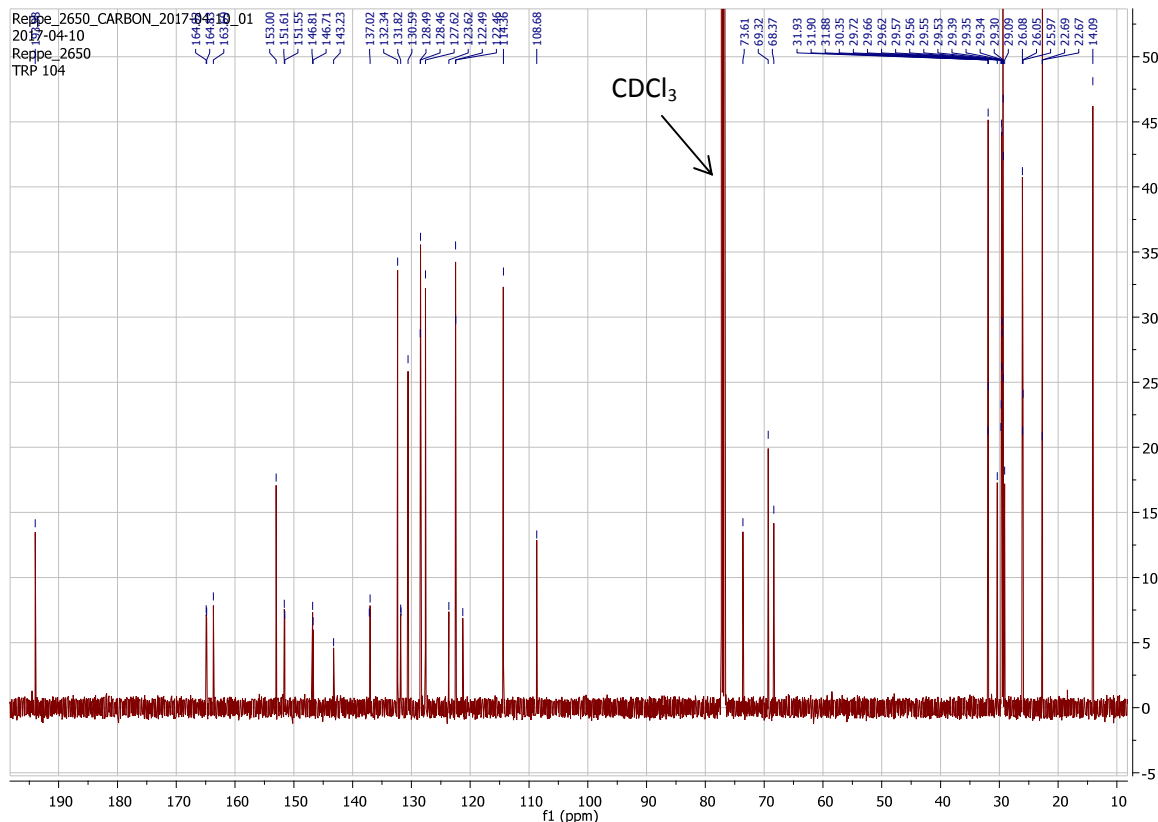


Figure S18.  $^{13}\text{C}$ -NMR spectrum of 3/10 (125 MHz,  $\text{CDCl}_3$ ).

## 5. References

---

- S1 A. Immirzi, B. Perini, *Acta Cryst.* **1977**, *A33*, 216–218.
- S2 X. Zeng, G. Ungar, *J. Mater. Chem. C* **2020**, *J. Mater. Chem. C*, doi:10.1039/D0TC00447B (2020)
- S3 R. A. Reddy, C. Tschierske, *J. Mater. Chem.* **2006**, *16*, 907–961.
- S4 Autorenkollektiv, *Organikum*, 21. Ed, Wiley-VCH, Weinheim, **2001**, pp. 480, 498
- S5 N. Miyaura, A. Suzuki, *Chem. Rev.* **1995**, *95*, 2457–2483.